THE JOURNAL OF BIOLOGICAL CHEMISTRY VOL. 283, NO. 14, pp. 8893–8901, April 4, 2008

Biophysical Characterization of *O*-Glycosylated CD99 Recognition by Paired Ig-like Type 2 Receptors*[S]

Received for publication, November 30, 2007, and in revised form, January 28, 2008 Published, JBC Papers in Press, January 30, 2008, DOI 10.1074/jbc.M709793200

Shigekazu Tabata[‡], Kimiko Kuroki[‡], Jing Wang[§], Mizuho Kajikawa[‡], Ikuo Shiratori[§], Daisuke Kohda[‡¶], Hisashi Arase[§¶], and Katsumi Maenaka[‡¶2]

From the [‡]Division of Structural Biology, Medical Institute of Bioregulation, Kyushu University, 3-1-1 Maidashi, Higashi-ku, Fukuoka 812-8582, the [§]Department of Immunochemistry, Research Institute for Microbial Diseases, and the [¶]World Premier International Immunology Frontier Research Center, Osaka University, Yamadaoka 3-1, Suita, Osaka 565-0871, and Solution Oriented Research for Science and Technology, Japan Science and Technology Agency, Saitama 332-0012, Japan

Paired Ig-like type 2 receptors (PILRs) are one of the paired receptor families, which consist of two functionally opposite members, inhibitory (PILRα) and activating (PILRβ) receptors. PILRs are widely expressed in immune cells and recognize the sialylated *O*-glycosylated ligand CD99, which is expressed on activated T cells, to regulate immune responses. To date, their biophysical properties have not yet been examined. Here we report the affinity, kinetic, and thermodynamic analyses of PILR-CD99 interactions using surface plasmon resonance (SPR) together with site-directed mutagenesis. The SPR analysis clearly demonstrated that inhibitory PILRα can bind to CD99 with low affinity ($K_d \sim 2.2$ μM), but activating PILRβ binds with ~40 times lower affinity ($K_d \sim 85$ μM). In addition to our previous mutagenesis study (Wang, J., Shiratori, I., Saito, T., Lanier, L. L., and Arase, H. (2008) *J. Immunol.* 180, 1686–1693), the SPR analysis showed that PILRα can bind to each Ala mutant of the two CD99 *O*-glycosylated sites (Thr-45 and Thr-50) with similar binding affinity to wild-type CD99. This indicated that both residues act as independent and equivalent PILRα binding sites, consistent with the highly flexible structure of CD99. On the other hand, it is further confirmed that PILRβ can bind the T50A mutant, but not the T45A mutant, indicating a recognition difference between PILRα and PILRβ. Kinetic studies demonstrated that the PILR-CD99 interactions show fast dissociation rates, typical of cell-cell recognition receptors. Thermodynamic analyses revealed that the PILRα-CD99 interaction is enthalpically driven with a large entropy loss ($-T\Delta S = 8.9$ kcal·mol^{-1}), suggesting the reduction of flexibility upon complex formation. This is in contrast to the entropically driven binding of selectins to sugar-modified ligands involved in leukocyte rolling and infiltration, which may reflect their functional differences.

Immune cell surface receptors are involved in both activating and inhibitory signaling, and their balance determines the functional responses of immune cells (1–4). Some of these receptor families have members with very similar extracellular regions responsible for ligand recognition but with different functions, activation and inhibition, due to the amino acid sequences of the transmembrane and intracellular regions. These receptor families are called "paired receptor families" and include human killer cell immunoglobulin (Ig)-like receptors (KIRs/CD158), human Leukocyte Ig-like receptors (LILRs/LIRs/ILTs/CD85), CD94/NKG2, and mouse Ly49.

Paired Ig-like type 2 receptors (PILRs)[3] are one of the paired receptor families and are composed of 1) inhibitory PILRα, which has the immune receptor tyrosine-based inhibitory motif that recruits a phosphatase to mediate the inhibition of immune responses, and 2) activating PILRβ, which has a positive lysine residue in the transmembrane region and associates with DAP12, harboring the immune receptor tyrosine-based activating motif (5–7). PILRs are expressed in immune cells, including natural killer cells, macrophages, and dendritic cells. Cellular-based assays revealed that PILRβ can induce the activation of natural killer cells and dendritic cells (7).

Our previous work identified the heavily *O*-linked glycosylated CD99 as a physiological PILR ligand (7). CD99 is a cell surface ligand on all leukocyte lineages, and it is especially highly expressed on activated T cells, where it may regulate the functional communication between PILR-expressing dendritic cell and CD99-expressing T cells. A recent report demonstrated that PILRs recognize two sialylated core1-type *O*-glycosylation sites of CD99 but both the core 2 branching and desialylation disturbed the PILR recognition (8). The extracellular region of PILR has one Ig-like domain (residue numbers 40–156) with the C-terminal stalk region. A Basic Local Alignment Search Tool (BLAST) analysis revealed that sialoadhesin (9), one of Siglec (sialic-acid-binding Ig-like lectins) receptors, which have an Ig fold and recognize sialic acid (Fig. 1), exhibits weak homology (~22% identity) with the Ig-like domain of PILRs, suggesting the possibility of a similar sugar binding mode between PILRs and Siglecs. On the other hand, the extracellular domains between PILRα and β are highly conserved (amino acid iden-

* The costs of publication of this article were defrayed in part by the payment of page charges. This article must therefore be hereby marked "*advertisement*" in accordance with 18 U.S.C. Section 1734 solely to indicate this fact.

[S] The on-line version of this article (available at http://www.jbc.org) contains supplemental Figs. S1 and S2 and Tables S1 and S2.

[1] Supported by the Ministry of Education, Science, Sports, Culture and Technology of Japan.

[2] To whom correspondence should be addressed. Tel.: 81-92-642-6969; Fax: 81-92-642-6764; E-mail: kmaenaka@bioreg.kyushu-u.ac.jp.

[3] The abbreviations used are: PILR, paired Ig-like type 2 receptor; SPR, surface plasmon resonance; MES, 4-morpholineethanesulfonic acid; BSA, bovine serum albumin.

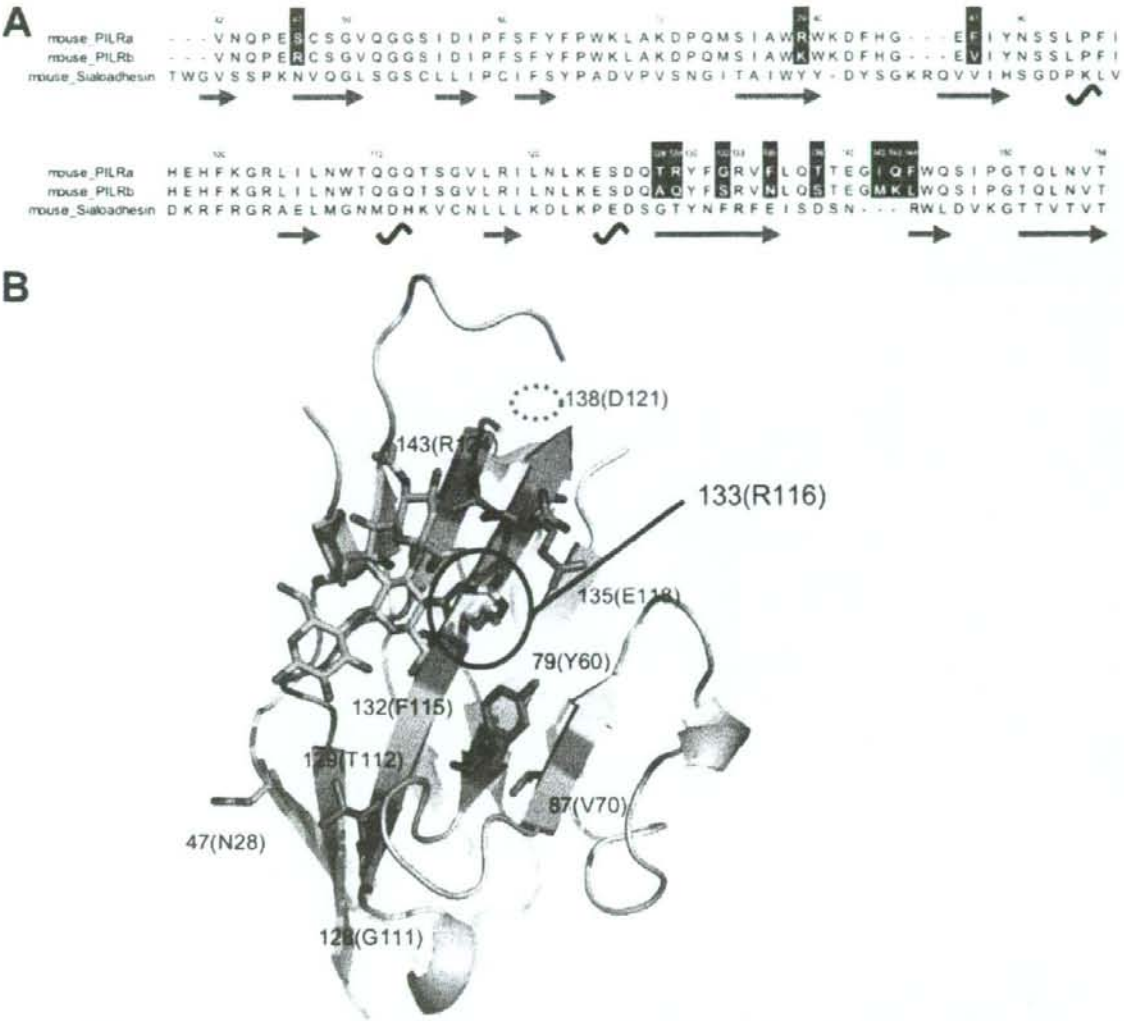

FIGURE 1. **Amino acid sequence alignment of PILRs with sialoadhesin and structure of sialoadhesin.** *A*, amino acid sequence alignments of PILRα and PILRβ with sialoadhesin. The *magenta characters* indicate the amino acid differences between the PILRs. Based on the crystal structure of sialoadhesin (9), the *brown arrows* and *blue twist lines* indicate the β-strands and 3_{10} helices, respectively. *B*, the schematic model presentation of the three-dimensional structure of sialoadhesin (PDB ID: 1QFO) (9), with mapping of the amino acid differences between PILRα and β (*magenta stick models*). The color coordination is the same as that in *A*. The *cyan stick model* indicates a sialyllactose bound onto sialoadhesin. The conserved arginine residue among the Siglec members and the PILRs is shown in a *yellow stick model*. The figure was produced using PyMol.

tity ~90% in the Ig-like domains). An immunoprecipitation experiment showed that the inhibitory PILRα can bind to CD99 more strongly than the activating PILRβ (7), suggesting the functional dominance of inhibitory PILRα, as in other paired receptor families, such as KIRs and CD94/NKG2.

A biophysical characterization of the properties of the PILR-CD99 interactions would yield important insights for understanding their physiological relevance. Here we report a comprehensive analysis of the kinetic and thermodynamic properties of the interactions by surface plasmon resonance and site-directed mutagenesis. We also compared the molecular mechanisms for the recognition of sugar-modified ligands by PILRs and selectins.

EXPERIMENTAL PROCEDURES

Production of Soluble V-set Domains of PILRα and PILRβ—The DNAs encoding the V-set domains of the extracellular regions (residues 40–156) of PILRα and PILRβ were amplified from the cDNAs obtained as described previously (7). The resultant fragments were digested with the restriction enzymes NdeI and HindIII and were ligated into pGMT7, creating the plasmids pGMPILRα and pGMPILRβ encoding PILRα and PILRβ, respectively. With regards to PILRβ, the C48S mutation

was additionally introduced by QuikChange (Stratagene), to avoid the formation of the disulfide-linked dimer. The plasmids were transformed into the *Escherichia coli* strain BL21(DE3)/RIL, and the cells were cultured in a 1 liter of 2YT medium (1.6 % Bacto-Tryptone, 1% yeast extract, and 0.5 % NaCl) with 100 mg/lliter ampicillin (Nacalai Tesque, Japan) at 310 K. When the A_{600} reached 0.6, isopropyl β-D-thiogalactopyranoside (Nacalai Tesque, Japan) was added for induction at a final concentration of 1 mM. The cells were induced for 6 h, and were harvested by centrifugation. The recombinant proteins accumulated as insoluble aggregates in inclusion bodies. The cell pellet was suspended in resuspension buffer (50 mM Tris-HCl, pH 8.0, 100 mM NaCl) and was centrifuged. The pellet was washed with Triton buffer (0.5% Triton X-100, 50 mM Tris-HCl, pH 8.0, 100 mM NaCl) and was centrifuged twice. The pellet was then suspended in resuspension buffer and was centrifuged to remove unnecessary detergent. The purified inclusion bodies were finally dissolved in guanidine buffer (6 M guanidine-HCl, 50 mM MES, NaOH, pH 6.5, 100 mM NaCl, 10 mM EDTA).

To refold the proteins, 20 mg of solubilized inclusion bodies was gradually diluted by the addition of refolding buffer (1 M L-arginine-HCl, 0.1 M Tris-HCl, pH 8.0, 2 mM EDTA) at 277 K. The resultant solution was stirred for 2 days and was concentrated to 5–10 ml by a VIVA FLOW system. The proteins were purified by gel filtration (HiLoad26/60 Superdex 75 pg, GE Healthcare).

Production of Soluble CD99s—The DNA fragments encoding the extracellular portions of CD99 and its mutants (CD99-T45A (Thr-45 → Ala), -T50A(Thr-50 → Ala), and -FM (full Ala mutations of all potential *O*-glycan sites)) were each cloned into the XhoI site of a modified pME18S expression vector, containing a mouse CD150 leader sequence at the N-terminal site and the Fc fragment of human IgG at the C-terminal one (8). The vector DNAs were transfected into 293T cells using polyethyleneimine, for transient expression. The supernatants were collected 96 h after the transfection, and the Fc-fused CD99s were purified with a protein A affinity column.

Binding Analysis Using SPR—PILRα and PILRβ were each dissolved in HBS-EP buffer (10 mM HEPES, pH 7.4, 150 mM NaCl, 3 mM EDTA, 0.005% Surfactant P20) (BIAcore AB). SPR experiments were performed with a BIAcore2000 (Biacore AB). All of the proteins were covalently immobilized on the CM5 sensor chip by amine-coupling using the standard amine coupling kit (BIAcore AB). For coupling the samples were injected at 50–100 μg/ml for 1–10 min in 10 mM sodium acetate, pH 4.5. Bovine serum albumin (BSA) was used as a negative control protein. All PILR injections were for 30 s, at a flow rate of 10 μl/min. The data were analyzed using BIAevaluation version 4.1 (Biacore AB) and ORIGIN version 7 (MicroCal Inc.) software. Equilibrium analyses determined K_d values by nonlinear curve fitting of the Langmuir binding isotherm.

For kinetics, all PILR injections were at a flow rate of 50 μl/min. The global fitting analysis using the 1:1 Langmuir binding model was simultaneously performed with the raw data for the association and dissociation phases at different concentrations of PILRα. Fitting was performed using BIAevaluation version 4.1.

Equilibrium analyses of PILRα were performed at five temperature points (10 °C, 15 °C, 20 °C, 25 °C, and 30 °C). The standard state Gibbs energy change upon binding was obtained from Equation 1:

$$\Delta G = RT \ln K_d \quad \text{(Eq. 1)}$$

where K_d is dissociation constant expressed in units of mol.l^{-1}, and R is the gas constant. The ΔG values of each data set were plotted against the temperatures, and were fitted with the nonlinear van't Hoff equation (Equation 2),

$$\Delta G = \Delta H - T\Delta S + \Delta C_p(T - 298.15) - \Delta C_p T \ln(T/298.15) \quad \text{(Eq. 2)}$$

where ΔH and ΔS are the binding enthalpy and entropy at 298.15 K, respectively, and ΔC_p is the heat capacity, which is assumed to be temperature-independent.

Glycan Array Binding Screening—The Fc-fused proteins of PILRα and PILRβ were prepared as previously reported in Wang *et al.* (8). Briefly, the proteins were produced in COS-7 cells by transient expression, similarly to the preparation of CD99s. The supernatants were collected 72 h after the transfection, and the purification was performed by a protein A affinity column. The glycan array screening was supported by the international established group, The Consortium for Functional Glycomics (detailed on the their website). A huge library of natural and synthetic glycans with amino linkers is covalently attached onto glass microscope slides via amide linkages, resulting in a printed glycan array. The Fc-fused PILRs (200 μg/ml) were incubated with the glycan microarray (version 3.0), including >300 sugars (see supplemental Tables S1 and S2). Then the Alexa Fluor 488-labeled goat anti-human IgG antibody (Molecular Probes) was used for the detection of the fluorescence if the proper binding occurred.

RESULTS

Expression and Purification of PILRs and CD99—The V-set Ig domains (residues numbers 40–156) of mouse PILRα and PILRβ were expressed in *E. coli* as inclusion bodies and were refolded *in vitro* by a dilution method (see details under "Experimental Procedures"). The refolded proteins migrated as monomers and were purified on size-exclusion columns (Fig. 2), and the final products showed high purity.

According to Wang *et al.* (8), the ectodomain of mouse CD99 fused with the Fc fragment of human IgG at the C-terminal site was expressed by a transient expression system, using 293T cells. The CD99 fusion protein was purified by chromatography on a protein-A column. It migrated as a 47-kDa species under reduced SDS-PAGE, and was used without further purification for binding studies (data not shown).

Differential Binding Activity Mediates CD99 Recognition by PILRs—The CD99 binding activity of the PILR ectodomains was analyzed by SPR. Each PILR was simultaneously injected (Fig. 3, *solid bar*) onto four flow cells containing sensor surfaces to which wild-type CD99 (CD99-WT) or BSA (negative control) had been immobilized by direct amine coupling. A greater response was observed with the injection of the inhibitory PILRα onto CD99-WT in comparison with that onto BSA, indi-

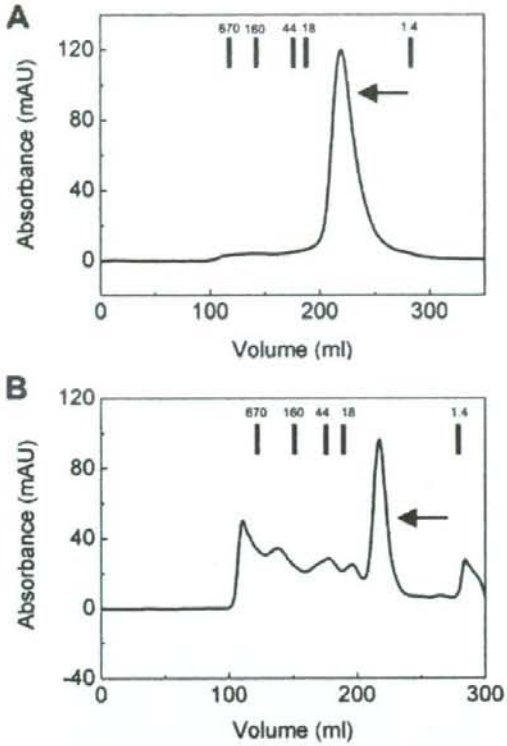

FIGURE 2. **Gel-filtration chromatography analysis of PILRs.** Chromatogram of PILRα (*A*) and PILRβ (*B*) on HiLoad26/60 Superdex 75-pg gel filtration column. The *arrows* indicate the peaks of the PILRs. The *bars* indicate the elution positions of the molecular mass markers (kilodaltons).

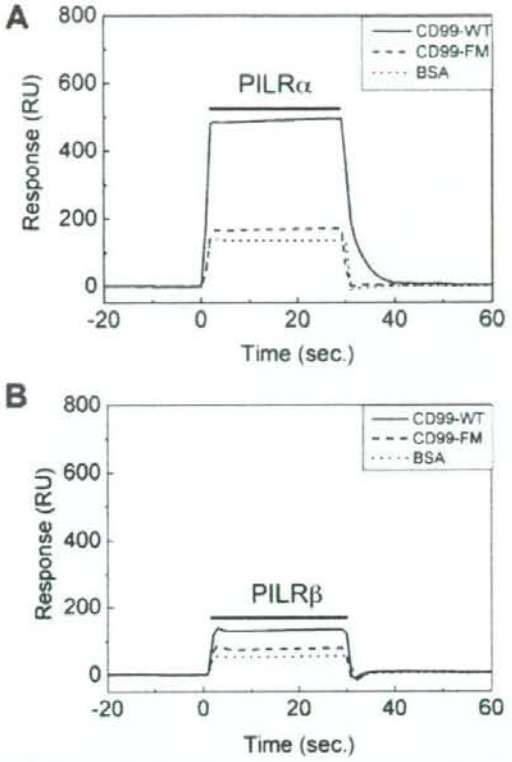

FIGURE 3. **Specific binding of PILRs to CD99s.** PILRα (*A*, 69 μM), or PILRβ (*B*, 95 μM) was injected (*solid bar*) at 25 °C. The difference between the responses of the BSA and CD99 flow cells represents the specific binding. *A*, PILRα binding to CD99-WT (*dashed line*), CD99-FM (*dotted line*), and BSA (*solid line*). *B*, PILRβ binding to CD99-WT (*dashed line*), CD99-FM (*dotted line*), and BSA (*solid line*).

cating specific binding to CD99-WT (Fig. 3*A*). In contrast, the activating PILRβ showed much lower binding responses to CD99-WT (Fig. 3*B*). Previous cellular-based assays revealed that the activating PILRβ regulates the CD99-transfected cells much less efficiently than the inhibitory PILRα (7). Therefore, the present binding study supports the differential binding affinities of PILRα and PILRβ.

The affinities of PILR binding to CD99 were determined by an equilibrium binding analysis. A range of concentrations of PILRα or PILRβ were injected through flow cells with immobilized CD99-WT or BSA as a control. The binding response was calculated by subtracting the equilibrium response in the control flow cell from the response in each flow cell. Conventional (Fig. 4) and Scatchard (Fig. 4, *inset*) plots of these binding data indicated that the interaction conforms to a simple 1:1 Langmuir binding model. The dissociation constant (K_d) for the PILRα-CD99 interaction was 2.2 μM at 25 °C (298.15 K), whereas that for the PILRβ-CD99 interaction was much lower, 85 μM. The results are summarized in Table 1. The PILRα-CD99 interaction showed low affinity within the range of typical cell-cell recognition events, but the PILRβ-CD99 interaction was at the lowest edge of the range (Table 2).

Two Equivalent PILRα Binding O-Glycan Sites—As described above, the previous cellular-based binding study using CD99 mutants (8) demonstrated that PILRα and PILRβ recognize CD99 modified with sialylated *O*-linked sugar. Here, we further performed the glycan array screening provided by The Consortium for Functional Glycomics (detailed on their website). The Fc-fused PILRα and PILRβ did not show significant binding to any sugar molecules on the glycan microarray (version 3.0), including >300 sugars, although PILRα showed subtle binding to α-Neu5Ac and Neu5Gcα (supplemental Figs. S1 and S2 and Tables S1 and S2). Especially, sialylated sugars such as Neu5Acα2→3Gal1→3GalNAc and Neu5Acα2→6Gal1→3GalNAc were not recognized by PILRs. In addition, the cellular-based competition assay indicated that neither Neu5Ac, NeuAcα2→3Gal, or NeuAcα2→6Gal competes with the PILR-CD99 interaction.[4] These results suggest that PILRs recognize more complicated structure rather than simple sugar molecules, which are sialylated *O*-linked sugars presumably together with a certain sugar modification and/or the peptide sequence specific to CD99.

Furthermore, Wang *et al.* (8) demonstrated that the two mutations, Thr-45 and Thr-50, of CD99 reduced the molecular

[4] J. Wang and H. Arase, unpublished observation.

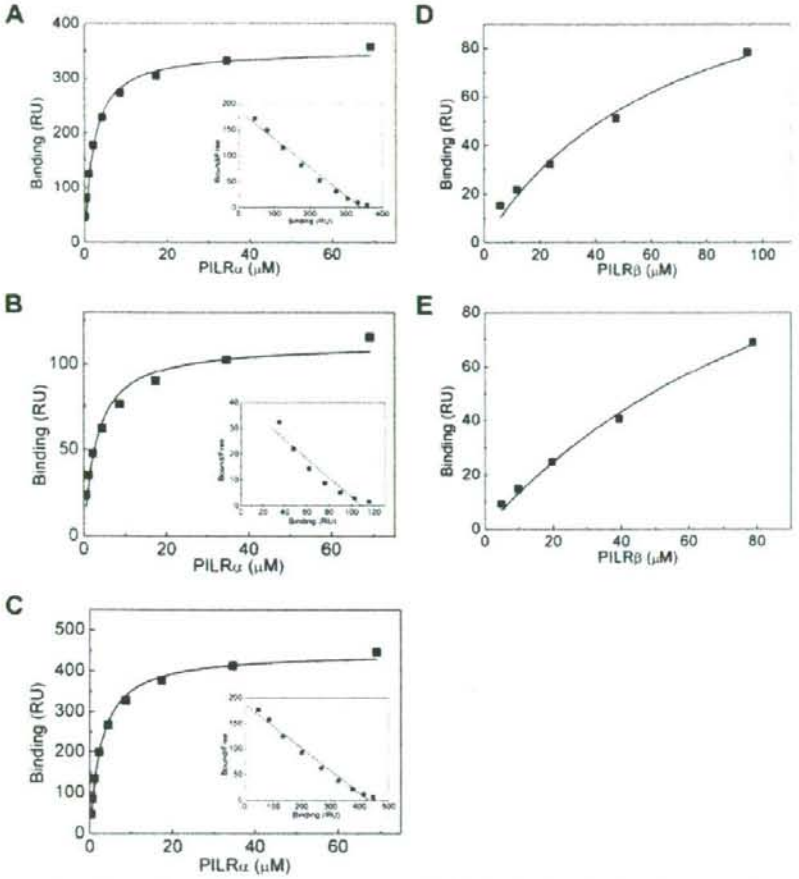

FIGURE 4. **Measuring the affinity of the PILR-CD99 interactions.** The affinities of the PILR-CD99 interactions were determined by equilibrium binding experiments. *A–C*, ten 2-fold dilutions of PILRα (69-0.13 μM) were injected over the CD99s, and the responses were plotted against the concentrations of injected PILRα protein. *A*, binding to CD99-WT (*closed squares*). *B*, binding to CD99-T45A. *C*, binding to CD99-T50A. *Inset*, Scatchard plots of the same data are shown. The *solid lines* are linear fits. *D* and *E*, five 2-fold dilutions of PILRβ (*D*: 95-5.9 μM, *E*: 79-4.9 μM) were injected over the CD99s. *D*, binding to CD99-WT (*closed squares*). *E*, binding to CD99-T50A. The coefficient determinations for the fittings are: *B* (PILRα-CD99-T45A), 0.969 (non-linear) and 0.956 (Scatchard); *D* (PILRβ-CD99-WT), 0.984 (non-linear); and *E* (PILRβ-CD99-T50A), 0.994 (non-linear). Errors for these fittings are reasonably small, <30% of K_d values.

TABLE 1
Binding affinities of the interactions between PILRs and CD99s at 25 °C

The values are means ± range derived from two experiments.

Analyte	Immobilized	K_d
		μM
PILRα	CD99-WT	2.2 ± 0.03
	CD99-FM	NB[a]
	CD99-T45A	3.3 ± 0.2
	CD99-T50A	2.8 ± 0.02
PILRβ	CD99-WT	85 ± 15
	CD99-FM	NB
	CD99-T45A	NB
	CD99-T50A	154 ± 37

[a] NB, no detectable binding.

weight to be essentially the same as the mutant whose potential *O*-glycosylation sites were all mutated to alanine, indicating that the two sites are only *O*-glycosylated. These two *O*-glycosylation sites, Thr-45 and Thr-50, are relevant for PILR recognition; however, the extent of the roles of these sites in the binding activity has been unclear. Therefore, we performed SPR binding studies of the inhibitory PILRα to the CD99 mutants. As expected, no specific responses were observed in the flow cell of the CD99 mutant with Ala replacements at all potential *O*-glycosylation sites (full mutations, CD99-FM) upon the injection of either PILRα or PILRβ (Fig. 3), confirming the previous result (8) that the *O*-glycosylation is necessary for PILR recognition. On the other hand, the single Ala mutation at two *O*-glycosylation sites (T45A and T50A) did not cause any reduction of PILRα binding in comparison with that of the CD99-WT (Fig. 4, *A–C*, and Table 1). This indicated that the two *O*-glycan sites are independent and equivalent for the PILRα recognition. In contrast, the PILRβ bound the T50A mutant with similar affinity as the CD99-WT (Fig. 4, *D* and *E*), but did not bind to the T45A mutant (data not shown), supporting the previous observation (8) that these binding sites are not equivalent for PILRβ recognition.

Binding Kinetics—The equilibrium binding data for both PILR-CD99-WT interactions indicated very fast kinetics (Fig. 3). The PILRβ-CD99-WT interaction shows quite low affinity with much faster kinetics, making it difficult to obtain the precise association and dissociation rates. Therefore, the detailed kinetic parameters of the PILRα-CD99-WT interaction were determined, by global fitting of the mono-exponential rate equations derived from the simple 1:1 Langmuir binding model to the SPR data. Fig. 5 illustrates the reasonable fitting to the data for PILRα binding to CD99-WT, which yielded the association and dissociation rate constants, summarized in Table 2. PILRα bound CD99 with typical association ($k_{on} = 3.9 \times 10^5\ M^{-1}\cdot s^{-1}$) and fast dissociation ($k_{off} = 1.2\ s^{-1}$) kinetics similar to those of the interactions of other cell-cell recognition receptors (Table 2). The amount of immobilized CD99-WT did not affect the kinetic parameters significantly (Table 2), indicating that mass transport and rebinding artifacts were not factors in this experiment. The good consistency between the kinetically derived K_d (Table 2) and the K_d determined by equilibrium binding (Table 1) provided further evidence that these kinetic parameters are correct.

TABLE 2

Kinetic parameters of the interactions between PILRα or PILRβ and CD99 at 25 °C

The association kinetic constant (k_{on}) and dissociation kinetic constant (k_{off}) were fitted simultaneously to the response data at several analyte concentrations. $K_d$kin values were obtained from global fitting. $K_d$eq values were obtained from equilibrium analyses.

Analyte	Immobilized CD99	k_{on}	k_{off}	$K_d$kin	$K_d$eq[a]
		$\times 10^5$ (M^{-1} s^{-1})	s^{-1}	μM	
PILRα	WT (700 RU)[b]	3.9	1.2	3.0	2.2 ± 0.03
	WT (3800 RU)	5.1	1.0	2.0	2.2 ± 0.03
PILRβ	WT (3800 RU)				85 ± 15
		k_{on}	k_{off}	K_d	References
		$\times 10^5$ (M^{-1} s^{-1})	s^{-1}	μM	
Other protein-protein interactions					
E-selectin	ESL-1	0.48	2.7	56	(17)
L-selectin	GlyCAM-1	>1	>10	108	(18)
P-selectin	PSGL-1	44	1.4	0.32	(19)
LILRB1D1D2	UL18	1.4	0.0028	0.0021	(27)
KIR2DL3	HLA-Cw7/DS11	2.1	1.1	5.2	(28)
CD8αα	MHC class I	≥1.0	≥18	~200	(29)
CD22	CD45	≥1.5	≥18	117	(21)
CD80	CTLA-4	9.4	0.43	0.46	(30)
CD80	CD28	6.6	1.6	2.4	(30)
FcγRIIa,IIb,III	hFc1	3.8–4.4	0.31–0.69	0.72–1.9	(31)
TCR	peptide-MHC	0.009–0.2	0.01–0.1	1–90	(10, 11)

[a] The values are means ± range derived from two experiments.
[b] RU, response unit(s).

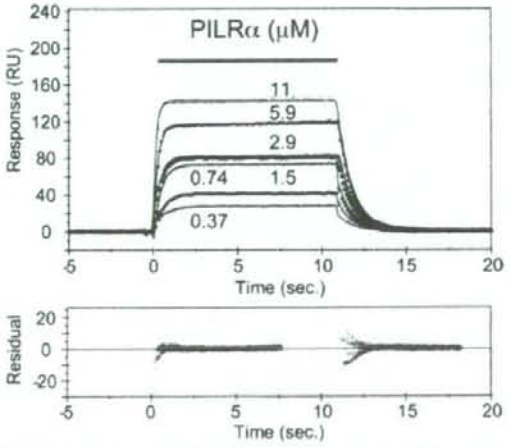

FIGURE 5. **Kinetic analysis of the PILRα-CD99 interaction.** PILRα at the indicated concentrations, was injected (*solid bar*) over CD99-WT (700 response units (*RU*)). Rate equations derived from the 1:1 binding model (A + B ↔ AB) were fitted to the association and dissociation phases of all six injections (global fitting). Residual errors from the fits are shown in the *bottom panel*.

Thermodynamic Properties of the PILRα-CD99 Interaction—Using the non-linear van't Hoff analysis (Equation 2 under "Experimental Procedures"), a series of binding experiments at a range of temperatures can simultaneously provide the following thermodynamic parameters: the enthalpy change (ΔH), the entropic change ($T\Delta S$) and the heat capacity (ΔC_p). Therefore, we determined the binding affinities of the PILRα-CD99-WT interaction at five temperatures (10, 15, 20, 25, and 30 °C). The reasonable fitting of the non-linear van't Hoff equation to the data produced the thermodynamic parameters (Fig. 6 and Table 3). The quite favorable enthalpic changes ($\Delta H \sim -16.6$ kcal·mol^{-1}), beyond the entropic loss ($T\Delta S \sim -8.9$ kcal·mol^{-1}), contribute to the binding energy ($\Delta G \sim 7.7$ kcal·mol^{-1}) at 25 °C, and thus the PILRα-CD99-WT interaction is completely enthalpic-driven. On the other hand, ΔC_p is within the range of values measured for other protein-protein interactions (-0.44 ± 0.07 kcal·mol^{-1}·K^{-1}) (Table 3).

We also performed the non-linear van't Hoff analyses for PILRα recognition of the T45A and T50A CD99 mutants (Fig. 6). Both mutants exhibited very similar enthalpically-driven thermodynamic parameters to the wild-type, thus confirming that Thr-45 and Thr-50 are both independent and equivalent for the PILRα recognition.

DISCUSSION

O-Glycosylation Sites—The present study clearly demonstrated that the *O*-glycans were indispensable for PILR recognition. This result agreed with the staining experiment with the CD99 mutant transfectants, which showed that non-*O*-glycosylated CD99 could not bind to either PILRα or PILRβ (8).

PILRα bound the CD99-WT and the CD99-T45A and -T50A mutants with similar affinities ($K_d \sim 2-4$ μM), indicating that the two *O*-glycosylation sites, Thr-45 and Thr-50, were independent and equivalent for PILRα recognition. These sites are located very close together (only four amino acids apart), but the amino acid sequence around the sites includes a high content of proline residues (NMKP$\underline{T}^{45}$PKAP$\underline{T}^{50}$PKKPS), and thus the protein structure around Thr-45 and Thr-50 is likely to be highly mobile to accomplish the independent behavior of PILRα recognition. It also suggested that the main recognition target for PILRα seems to be the *O*-glycan, rather than the protein. Our previous cellular-based study (8) demonstrated that SDS-treated CD99 still has binding activity to the PILRα-Ig fusion protein, supporting the idea that PILRα mainly recognizes the *O*-glycan part of CD99.

On the other hand, the previous cellular and present binding studies showed that PILRβ-CD99 binding is not affected by the T50A mutation but is abolished by the T45A mutation (8). The amino acid sequences around Thr-45 and Thr-50 are very similar, with the common motif PTPK (NMK$\underline{PT}^{45}$PKA$\underline{PT}^{50}$PKKPS, underlined), implying the duplicated sequence. Thus, the amino acid sequence at the N-terminal side, rather than that at the C-terminal side, of

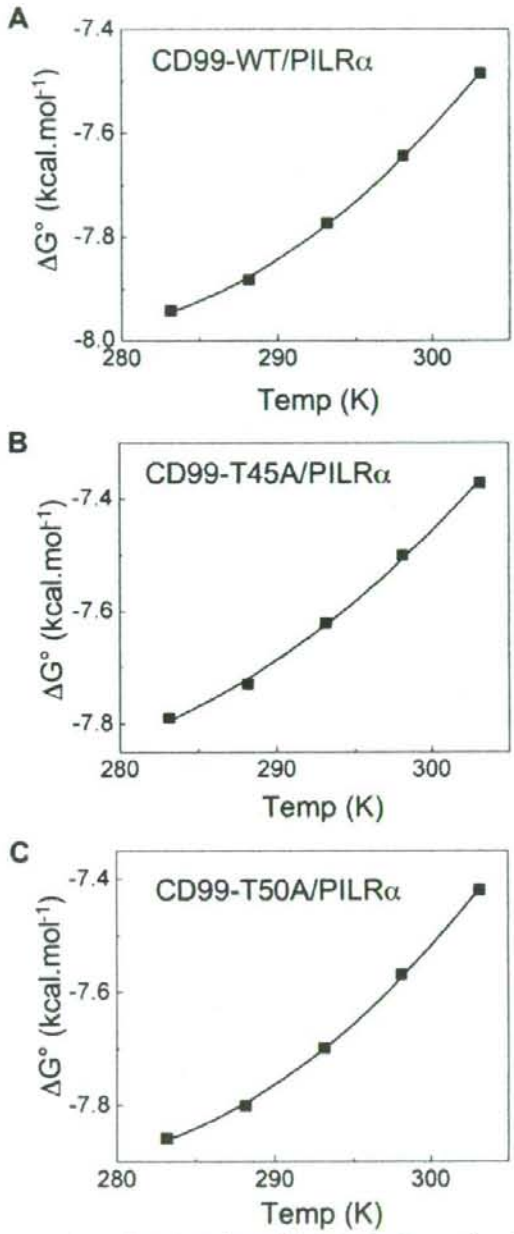

FIGURE 6. **Thermodynamic analyses of the PILRα-CD99 interactions.** The dissociation constants (K_d) for the PILRα-CD99 interactions were measured at five temperatures (10–30 °C) and were converted into the standard free energy of binding ($\Delta G°$): CD99-WT (*A*), -T45A (*B*), and -T50A (*C*). Values for the enthalpic (ΔH) and standard entropic ($-T\Delta S°$) changes (at 25 °C) and the specific heat capacity (ΔC_p) were determined by fitting the non-linear van't Hoff equation to these data.

the sialylated *O*-glycosylation site seems to be important for PILRβ recognition. However, further investigations, especially a structural study of the recognition of the *O*-glycan and its attached polypeptide by PILR, will be necessary to clarify the functional characteristics. Taken together, these results indicate that both PILRs recognize the flexible *O*-glycosylated sites of CD99, even though there are differences in the peptide dependence.

Kinetic Characteristics—PILRα bound to CD99 with a typical association rate constant ($k_{on} = 3.9 \times 10^5\ M^{-1}\cdot s^{-1}$) and dissociated with a fast dissociation rate constant ($k_{off} = 1.2\ s^{-1}$). These kinetic parameters indicated that PILRα binds to CD99 with fast kinetics, within the range of typical cell-cell recognition events (Tables 1 and 2). PILRβ also showed fast binding kinetics, although the specific parameters were not determined. This indicates that the interactions between PILR and CD99 are unstable, and the fast dissociation rates promote the exchange of PILR-CD99 interactions, suggesting that the formation of appropriate multivalent complexes at the cell-cell interface is required for signaling. In a later section, we will discuss the functional consequences of the differences in the sugar-modified ligand recognition between PILRs and selectins.

Thermodynamic Characteristics—The binding of PILRα to CD99 was characterized by quite favorable enthalpic changes beyond the large entropic loss, in contrast to entropically and enthalpically driven binding observed in typical protein-protein interactions, including cell-surface receptor-ligand interactions, such as the KIR-MHC interaction (Fig. 7 and Table 3). Unfavorable entropic changes upon complex formation are mainly due to the reduction in the conformational flexibility and/or the trapping of water molecules at the binding interface. The enthalpically driven interactions include the TCR-MHC (10–15) and gp120-CD4 (16) interactions. These interactions exhibit slow k_{on} values, suggesting that large, time-consuming conformational adjustments are necessary to achieve the proper binding state. However, the PILR-CD99 interaction exhibited a relatively fast association rate. Furthermore, the heat capacity change (ΔC_p) is not very small, ~440 $cal\cdot mol^{-1}\cdot K^{-1}$, but it is much less than that in gp120-CD4 binding (1200–1800 $cal\cdot mol^{-1}\cdot K^{-1}$), indicating that only small conformational changes may be required. On the other hand, core 1 sugars of CD99 might be linear compared with the branched core 2 sugars and thus more flexible than the branched sugars like sialyl Lewis sugars and ligands of selectins, which would contribute to the entropy penalty of the CD99-PILR interaction. Thus, the PILRs probably capture the highly flexible structure of the *O*-glycan and its attached peptide of CD99 with some degree of conformational fixation and/or trapping of water molecules.

Comparison with Selectin-Ligand Interactions—The selectin family on leukocytes recognizes sugar-modified ligands on the vascular endothelium to facilitate leukocyte tethering and rolling. Binding studies revealed that the selectin-ligand interactions (E-selectin-ESL-1 (17), L-selectin-GlyCAM-1 (18), and P-selectin-PSGL-1 (19)) exhibit fast kinetics and are basically entropically driven (Tables 2 and 3, and Fig. 7). As described above, this is in sharp contrast to the enthalpically driven PILR-CD99 binding. The sugar-modified ligands have intrinsically high conformational entropy derived from the *O*-linked oligosaccharides, and their fixation upon protein binding contributes to unfavorable entropic changes, as observed in many sug-

TABLE 3
Thermodynamic parameters of the interaction between PILRα and CD99s at 25 °C

Analyte	Immobilized	References	ΔG	ΔH	$-T\Delta S$	ΔC_p
				kcal·mol⁻¹		*kcal·mol⁻¹·K⁻¹*
PILRα	CD99-WT[a]	This study	−7.7 ± 0.03	−16.6 ± 0.2	8.9 ± 0.2	−0.44 ± 0.07
	CD99-T45A[a]	This study	−7.5 ± 0.00	−15.3 ± 0.2	7.8 ± 0.2	−0.28 ± 0.03
	CD99-T50A[a]	This study	−7.6 ± 0.00	−16.0 ± 0.1	8.5 ± 0.1	−0.37 ± 0.02
E-selectin	ESL-1	(17)	−5.7	−0.9	−4.8	
FcγRIIa, IIb	hFc1	(31)	−7.9 to −8.3	−4.4 to −6.4	−1.9 to −3.3	−0.22 to −0.43
FcγRIII	hFc1	(31)	−8.0	−15.4	7.4	−0.7
KIR2DL3	HLA-Cw7	(28)	−7.2	−4.1	−3.1	−0.1
CD22	CD45	(21)	−5.1	−10.1	5.0	−0.08
NKG2D	Rael	(32)	−8.6	−5.2	−3.4	
NKG2D	H60	(32)	−10.5	−23.6	13.1	
TCR	MHC	(10–15)	−7.1 ± 0.6	−14.6 ± 5.4	7.1 ± 5.7	−0.62 ± 0.37

[a] The values are means ± range derived from two experiments.

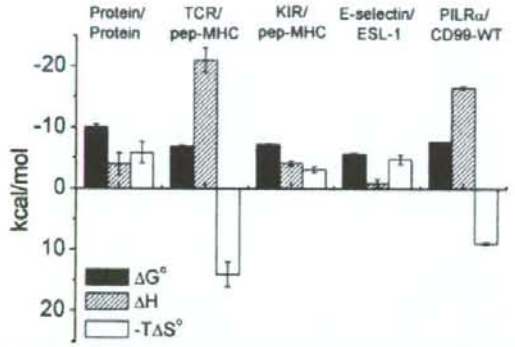

FIGURE 7. **Comparison of the thermodynamic properties of several protein-protein interactions (at 25 °C).** The values for protein-protein interactions (excluding antibody-antigen interactions) are the mean ± S.D. of 30 distinct interactions taken from Stites (26).

ar-lectin interactions (20). Thus, the PILR-CD99 interactions presumably adopt such a recognition mode. On the other hand, the selectin-ligand recognition seems to avoid strong conformational fixation and/or entrapment of waters at the binding interface. It seems that fast kinetics and smaller conformational rearrangements upon selectin-ligand complex formation would be beneficial for the tethering and rolling of leukocytes, which move quickly in the bloodstream. In contrast, PILRs might utilize a more static binding mechanism to achieve proper signaling in a localized area, such as the lymph node, where PILR-expressing dendritic cell and CD99-expressing T cells interact.

Comparison with the Siglec Family—As described in the introduction, a BLAST analysis revealed that sialoadhesin exhibits weak homology (~22% identity) with PILRs (Fig. 1*B*). PILRs harbor the most important arginine residue for sialic acid recognition, conserved in Siglec family members. The mutation of the conserved arginine residue directly recognizing sialic acid (Arg-133 in PILRs/Arg-116 in sialoadhesin) abolished the PILR-CD99 interactions,[4] suggesting that the PILRs have a similar sugar binding mode as the Siglecs. However, PILR seems not to recognize simple sialylated sugars unlike Siglecs. Furthermore, genome localization of PILR is not linked to that of Siglec family. Therefore, PILR seems to be a relative but not a member of Siglecs.

CD22 is a member of the Siglec family and interacts with sialylated glycans on several molecules such as CD45, in an enthalpy-driven process (21), similarly to the PILR-CD99 interactions. However, PILRs do not recognize CD45-expressing CD4 T cells (8), and thus PILRs at least have recognition specificity different from CD22 even though sialylated sugars are involved in the ligand recognition by these receptors. It would be interesting to clarify the similarity and difference of these recognition systems by further investigation.

Functional Differences between PILRα and PILRβ—Previous studies of the recognition characteristics of paired receptor families clarified the tendency that the inhibitory receptor has a higher affinity than the activating one, such as CTLA4/CD28, KIRs, and CD94/NKG2 (22). The proposed physiological reason for this is that inhibitory receptor interactions should overcome activating ones for immune cells, such as T and natural killer cells, so that they are inactive toward normal cells unless the activation is truly necessary. The present binding study revealed that the PILR family also exhibits the same differential binding properties to regulate immune cells as the above-mentioned immune cell surface receptors.

The amino acid residue differences between PILRα and PILRβ are localized within the C terminus (Fig. 1*A*). As described above, based on an amino acid sequence alignment with other Siglecs, these residues seem to constitute a part of the sugar recognition site (Fig. 1*B*). Thus, it is reasonable for these amino acid changes to significantly affect the binding affinity and specificity of PILRs to CD99.

There exists difference in recognition of the *O*-glycan mutated CD99s between PILRα and PILRβ. Single mutation at Thr-45 or Thr-50 did not affect the PILRα recognition but did for PILRβ binding. We have shown that both the single mutation (Thr-45 or Thr-50) reduced the killing activity of natural killer cells expressing PILRβ (8), indicating that the *O*-linked sugar modifications at Thr-45 and Thr-50 are regulating immune receptor tyrosine-based activating motif-mediated signals of PILRβ.

Weak binding affinity of PILRβ to CD99 was observed, and thus PILRβ may have other physiologically relevant roles. Arase *et al.* (23) proposed that some of the activating members of paired receptors may be reserved for surveying non-self ligands related to infectious diseases. For example, the mouse cytomegalovirus major histocompatibility complex class I-like molecule, m157, can bind to the activating Ly49 receptor, Ly49H, resulting in the acquirement of resistance to cytomegalovirus (24, 25). In a similar manner, PILRβ may have other ligands

derived from viruses, bacteria, etc. to achieve resistance to infectious diseases.

Functional Implication of O-Linked Sugar Modification of CD99—Activated lymphocytes express CD99. The intrinsic core 2 branching enzyme, core 2 β-1,6-*N*-acetylglucosaminyltransferase, expressed in B cells controls the generation of the B220 epitope on CD45. We have recently shown that PILRs recognize activated $B220^-$ T cells but not activated $B220^+$ B cells, even though both cells express CD99 (8). Because PILRs are expressed on antigen-presenting cells, this result suggested that *O*-linked sugar modifications generated by intrinsic core 2 β-1,6-*N*-acetylglucosaminyltransferase on lymphocytes control the PILR recognition, conferring the regulatory role of the CD99-PILR interactions on the innate and acquired immunity.

Conclusion—In this report, we showed that PILRs bind *O*-glycosylated CD99 with low affinities and fast kinetics, which are typical for cell-cell recognition receptors. The mutagenesis study revealed that PILRs recognize the flexible *O*-glycosylated sites of CD99, even though differential peptide dependence exists. The thermodynamic analysis showed unfavorable entropic changes upon PILR-CD99 complex formation, suggesting that PILRs capture the highly mobile CD99 structure with some degree of conformational fixation and/or trapping of water molecules. This is in contrast to the entropically driven selectin-ligand interactions, which are involved in the tethering and rolling of leukocytes in the bloodstream.

Acknowledgments—We thank Dr. David F. Smith for glycan array analysis and Dr. Lewis L. Lanier for helpful comments.

REFERENCES

1. Lanier, L. L. (2001) *Nat. Immunol.* **2,** 23–27
2. Smith, H. R., Idris, A. H., and Yokoyama, W. M. (2001) *Immunol. Rev.* **181,** 115–125
3. Moretta, A., Bottino, C., Vitale, M., Pende, D., Cantoni, C., Mingari, M. C., Biassoni, R., and Moretta, L. (2001) *Annu. Rev. Immunol.* **19,** 197–223
4. Diefenbach, A., and Raulet, D. H. (2003) *Curr. Opin. Immunol.* **15,** 37–44
5. Fournier, N., Chalus, L., Durand, I., Garcia, E., Pin, J. J., Churakova, T., Patel, S., Zlot, C., Gorman, D., Zurawski, S., Abrams, J., Bates, E. E., and Garrone, P. (2000) *J. Immunol.* **165,** 1197–1209
6. Mousseau, D. D., Banville, D., L'Abbe, D., Bouchard, P., and Shen, S. H. (2000) *J. Biol. Chem.* **275,** 4467–4474
7. Shiratori, I., Ogasawara, K., Saito, T., Lanier, L. L., and Arase, H. (2004) *J. Exp. Med.* **199,** 525–533
8. Wang, J., Shiratori, I., Saito, T., Lanier, L. L., and Arase, H. (2008) *J. Immunol.* **180,** 1686–1693
9. May, A. P., Robinson, R. C., Vinson, M., Crocker, P. R., and Jones, E. Y. (1998) *Mol. Cell* **1,** 719–728
10. Willcox, B. E., Gao, G. F., Wyer, J. R., Ladbury, J. E., Bell, J. I., Jakobsen, B. K., and van der Merwe, P. A. (1999) *Immunity* **10,** 357–365
11. Boniface, J. J., Reich, Z., Lyons, D. S., and Davis, M. M. (1999) *Proc. Natl. Acad. Sci. U. S. A.* **96,** 11446–11451
12. Davis-Harrison, R. L., Armstrong, K. M., and Baker, B. M. (2005) *J. Mol. Biol.* **346,** 533–550
13. Lee, J. K., Stewart-Jones, G., Dong, T., Harlos, K., Di Gleria, K., Dorrell, L., Douek, D. C., van der Merwe, P. A., Jones, E. Y., and McMichael, A. J. (2004) *J. Exp. Med.* **200,** 1455–1466
14. Garcia, K. C., Radu, C. G., Ho, J., Ober, R. J., and Ward, E. S. (2001) *Proc. Natl. Acad. Sci. U. S. A.* **98,** 6818–6823
15. Anikeeva, N., Lebedeva, T., Krogsgaard, M., Tetin, S. Y., Martinez-Hackert, E., Kalams, S. A., Davis, M. M., and Sykulev, Y. (2003) *Biochemistry* **42,** 4709–4716
16. Myszka, D. G., Sweet, R. W., Hensley, P., Brigham-Burke, M., Kwong, P. D., Hendrickson, W. A., Wyatt, R., Sodroski, J., and Doyle, M. L. (2000) *Proc. Natl. Acad. Sci. U. S. A.* **97,** 9026–9031
17. Wild, M. K., Huang, M. G., Schulze-Horsel, U., van der Merwe, P. A., and Vestweber, D. (2001) *J. Biol. Chem.* **276,** 31602–31612
18. Nicholson, M. W., Barclay, A. N., Singer, M. S., Rosen, S. D., and van der Merwe, P. A. (1998) *J. Biol. Chem.* **273,** 763–770
19. Mehta, P., Cummings, R. D., and McEver, R. P. (1998) *J. Biol. Chem.* **273,** 32506–32513
20. Dam, T. K., and Brewer, C. F. (2002) *Chem. Rev.* **102,** 387–429
21. Bakker, T. R., Piperi, C., Davies, E. A., and Merwe, P. A. (2002) *Eur. J. Immunol.* **32,** 1924–1932
22. Vales-Gomez, M., Reyburn, H., and Strominger, J. (2000) *Hum. Immunol.* **61,** 28–38
23. Arase, H., and Lanier, L. L. (2002) *Microbes Infect.* **4,** 1505–1512
24. Arase, H., Mocarski, E. S., Campbell, A. E., Hill, A. B., and Lanier, L. L. (2002) *Science* **296,** 1323–1326
25. Adams, E. J., Juo, Z. S., Venook, R. T., Boulanger, M. J., Arase, H., Lanier, L. L., and Garcia, K. C. (2007) *Proc. Natl. Acad. Sci. U. S. A.* **104,** 10128–10133
26. Stites, W. E. (1997) *Chem. Rev.* **97,** 1233–1250
27. Chapman, T. L., Heikeman, A. P., and Bjorkman, P. J. (1999) *Immunity* **11,** 603–613
28. Maenaka, K., Juji, T., Nakayama, T., Wyer, J. R., Gao, G. F., Maenaka, T., Zaccai, N. R., Kikuchi, A., Yabe, T., Tokunaga, K., Tadokoro, K., Stuart, D. I., Jones, E. Y., and van der Merwe, P. A. (1999) *J. Biol. Chem.* **274,** 28329–28334
29. Gao, G. F., Willcox, B. E., Wyer, J. R., Boulter, J. M., O'Callaghan, C. A., Maenaka, K., Stuart, D. I., Jones, E. Y., Van Der Merwe, P. A., Bell, J. I., and Jakobsen, B. K. (2000) *J. Biol. Chem.* **275,** 15232–15238
30. van der Merwe, P. A., Bodian, D. L., Daenke, S., Linsley, P., and Davis, S. J. (1997) *J. Exp. Med.* **185,** 393–403
31. Maenaka, K., van der Merwe, P. A., Stuart, D. I., Jones, E. Y., and Sondermann, P. (2001) *J. Biol. Chem.* **276,** 44898–44904
32. O'Callaghan, C. A., Cerwenka, A., Willcox, B. E., Lanier, L. L., and Bjorkman, P. J. (2001) *Immunity* **15,** 201–211

CONCISE COMMUNICATION

Reciprocal recognition of an HLA-Cw4-restricted HIV-1 gp120 epitope by $CD8^+$ T cells and NK cells

Hathairat Thananchai[a,b,*], Tariro Makadzange[b,*], Katsumi Maenaka[c], Kimiko Kuroki[c], Yanchun Peng[b], Chris Conlon[d], Sarah Rowland-Jones[b,*] and Tao Dong[b,*]

Objectives: The HIV-1 Nef protein selectively downregulates human leukocyte antigen (HLA)-A and HLA-B but not HLA-C molecules on the surface of infected cells. This allows HIV-infected cells to evade recognition by most cytotoxic T lymphocytes (CTLs) and natural killer (NK) cells. We investigated the recognition of an HLA-Cw4-restricted HIV-1 gp120 epitope SFNCGGEFF (SF9) and its variant SFNCGGEFL (SL9) by T cells and NK receptors.

Design and method: Recognition of HIV-1 gp120 peptides (SF9 and SL9) by T-cell clones was measured by staining with HLA-Cw4-peptide tetrameric complexes and cytolytic assays using target cell pulsed with either peptides. KIR2DL1 binding to these two peptides was measured using surface plasmon resonance and tetramer staining of an NK cell line.

Result: CTLs could recognize SF9 better than the variant SL9, as shown by both tetramer staining and cytolytic assays. Intriguingly, an HLA-Cw4 tetramer folded with the 'escape' variant SL9 could bind to KIR2DL1 on NK cell lines with higher affinity than HLA-Cw4-SF9. The binding of KIR2DL1 to its ligand results in inhibition of NK cell function. Our results indicate that the HIV-1 gp120 variant peptide SL9 could potentially escape both from NK cell and CTL recognition by increasing its affinity for KIR2DL1 binding.

Conclusion: These data suggest that HIV-1 can acquire mutations that are capable of escaping from both CTL and NK cell recognition, a phenomenon we have termed 'double escape'.

AIDS 2009, **23**:189–193

Keywords: AIDS, cytotoxic T cells, human, natural killer cells

[a]Department of Microbiology, Faculty of Medicine, Chiang Mai University, Chiang Mai, Thailand, [b]Weatherall Institute of Molecular Medicine, John Radcliffe Hospital, Headington, Oxford, UK, [c]Division of Structural Biology, Medical Institute of Bioregulation, Kyushu University, Maidashi, Higashi-ku, Fukuoka, Japan, and [d]Nuffield Department of Medicine, John Radcliffe Hospital, Headington, Oxford, UK.

Correspondence to Sarah Rowland-Jones and Tao Dong, MRC Human Immunology Unit, Weatherall Institute of Molecular Medicine, John Radcliffe Hospital, Oxford, OX3 9DS, UK.

Tel: +44 1865 222462; fax: +44 1865 222502; e-mail: tao.dong@imm.ox.ac.uk, sarah.rowland-jones@ndm.ox.ac.uk

* Contributed equally to the work in this manuscript.

Received: 28 August 2008; revised: 8 October 2008; accepted: 22 October 2008.

DOI:10.1097/QAD.0b013e32831fb55a

Introduction

Cytotoxic T lymphocytes (CTLs) play a central role in the control of persistent human immunodeficiency virus type 1 (HIV-1) infection [1,2]. However, HIV-1 employs several mechanisms for evading the potent CTL response that develops soon after infection [3]. One important mechanism of viral immune evasion is the selective downmodulation of cell surface human leukocyte antigen class I (HLA class I) molecules by HIV-1 nef [4,5], which leads to protection of infected cells from CTL killing. Downregulation is selective for HLA class I A and B molecules, so infected cells continue to express HLA-C, which reduces their vulnerability to natural killer (NK) cell recognition [6]. Evasion also occurs by mutation of the epitopes recognized by CTLs, which can lead to failure of the epitope to be generated by antigen processing, to bind to the HLA class I molecule or to be recognized by the T-cell receptor (TcR) of the responding CTL [1].

NK cells are a crucial component of the innate immune response to certain tumors and infections. NK cells can recognize HLA class I molecules through killer immunoglobulin-like receptors (KIRs) expressed on the cells surface. The engagement of inhibitory KIRs by their HLA class I ligands can prevent killing by NK cells [7,8]. KIR expression is highly variable on NK cells [9]; in general, KIR2D molecules tend to interact with HLA-C, whereas KIR3D interact with HLA-A and HLA-B [7,8,10]. We have recently demonstrated that the interaction between KIR3DL1 and its HLA ligands is exquisitely sensitive to variation in the KIR3DL1 allotypes, the HLA molecules and the nature of the bound peptide [11]. This raises the possibility that epitope peptide variants generated in the course of HIV-1 evolution under CTL selective pressure in the infected host could differ in their recognition by specific KIR molecules.

HLA-C-restricted cytotoxic T-cell responses to HIV proteins have been described in HIV-1-infected individuals [12,13] and in some patients, the HLA-Cw4-restricted response to a peptide from gp120 (SF9) may represent the dominant CTL response (Makadzange *et al.*, in preparation). The impact of HIV-1 Nef on HLA-A and B expression may lead to HLA-C-restricted responses playing a particularly important role in HIV-1 infection. Consistent with this hypothesis is the recent observation that a polymorphism associated with the increased expression of HLA-C is associated with delayed disease progression in HIV-1 infection [14]. Alteration of NK cell phenotype and function during the course of HIV infection has been reported [15,16]. HLA-Cw4 can also serve as a ligand for KIR2DL1 [7,8], raising the possibility that variant peptides generated in response to HLA-Cw4-restricted CTL pressure may have altered interaction with the KIR2DL1 ligand. In this study, we evaluated the interaction between KIR2DL1 and the HLA-Cw4-restricted CTL HIV-1 gp120 epitope SFNCGGEFF (SF9), together with its naturally occurring variant SFNCGGEFL (SL9).

Materials and methods

Study cohort

Blood samples were obtained from HIV-1-infected individuals enrolled in an HIV clinic in Oxford, United Kingdom. Human subject approval was given by the Central Oxford Regional Ethics committee. Informed consent was obtained from participants.

Generation of cytotoxic T-lymphocyte clones and natural killer lines

CTL lines and clones were generated as previously described [17]. NK lines were generated as previously described [11].

Surface plasmon resonance

HLA-Cw4 monomers were made as previously described and folded with the following peptides: QYDDAVYKL (QL9), representing a consensus Cw4-binding peptide [18], SFNCGGEFF (SF9) and SFNCGGEFL (SL9). Surface plasmon resonance studies were performed using a BIAcoreTM 2000 (BIAcore AB, St Albans, UK) as previously described [17]. Experiments were performed at 25°C. HEPES buffered saline-EP (HBS-EP) buffer was used as the running buffer.

K_D values and kinetic measurements were obtained either by Scatchard plots or by curve fitting of the data to the Langmuir binding isotherm. All analysis was done with BIAevaluation 3.2 RCI software (BIAcore AB) and graphs were produced with Origin software (version 5; Microcal Software, Northampton, Massachusetts, USA).

Tetramer staining

CTL clones or NK cell lines were stained with a panel of peptide-major histocompatibility complex (MHC) class I tetramer complexes as previously described [17]. For blocking experiments, cells were incubated on ice with anti-KIR2DL1 (HP3E4) or isotype control antibody for 30 min before adding the tetramers

^{51}Cr release cytotoxicity assay

Target cell lines (721.221 and HLA-Cw4 transfectant) were labeled with 100 μl of $Na^{51}CrO_4$ (Amersham International, Amersham Biosciences, Little Chalfont, Buckinghamshire, UK) for 1 h at 37°C. 721.221-expressing HLA-Cw4 were pulsed with various concentrations of HIV peptides. Effector and target cells were incubated at 37°C for 4 h. Specific lysis was calculated by using the following formula: percentage specific lysis = [(experimental − spontaneous lysis)/(maximum − spontaneous lysis)] × 100%.

Results

The HIV-1 gp120 epitope variant SL9 escapes recognition by human leukocyte antigen-Cw4-restricted cytotoxic T lymphocyte clones

The peptide SFNCGGEFF (SF9) represents the consensus sequence of the HLA-Cw4-restricted HIV-1 gp120 epitope in A, B and D clade strains of HIV-1. The TF9 (TFNCGGEFF) and SL9 (SFNCGGEFL) variants have been identified in HIV-1 isolates listed on the Los Alamos HIV Sequence database (http://www.hiv.lanl.gov). These variants were also found in viral sequences from HIV-1-infected Kenyan individuals in our study (Makadzange *et al.*, in preparation). HLA-Cw4-restricted CTL generated from HIV-1-infected individuals recognized the SF9 peptide with high affinity as shown by their ability to kill target cells pulsed with low peptide concentrations. In contrast, lysis of targets pulsed with the SL9 peptide was only observed at an unphysiologically high peptide concentration (10^{-5} mol/l). The recognition of variant peptide dramatically decreased at 10^{-6} mol/l peptide concentration (Fig. 1a and b).

Human leukocyte antigen-Cw4 refolded with the SL9 peptide bind to KIR2DL1 with high affinity

HLA-Cw4 is also recognized by KIR2DL1, an inhibitory receptor on NK cells. We studied the binding of HLA-Cw4 folded with the HIV-1 gp120 peptide to KIR2DL1. The relative importance of class I-associated peptides in recognition differs between TcR and KIR molecules. Specific recognition of MHC peptide by a TcR depends largely on the peptide sequence; in contrast, minimal interactions are observed between the peptide and KIR2DL1 [18]. Nevertheless, KIR recognition of HLA class I molecules does show some dependence on the bound peptide sequence [10,11], but direct contacts are limited to the peptide main chain at its COOH-terminal end. A previous study by Rajagopalan and Long [19] showed that KIR2DL1 did not interact with HLA-Cw4 bound to the SF9 peptide. Thus, we investigated whether the naturally occurring variants at carboxy terminus, such as SL9, could be recognized by KIR2DL1.

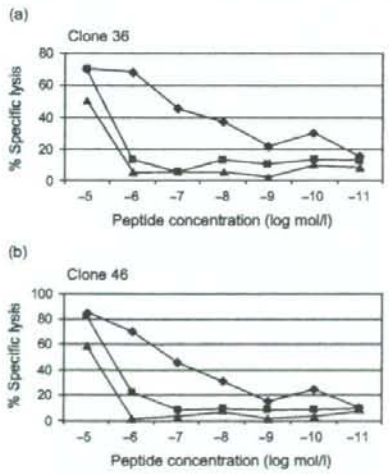

Fig. 1. Recognition of human leukocyte antigen (HLA)-Cw4 gp120 epitopes by HLA-Cw4-restricted cytotoxic T lymphocyte (CTL) clones. Two HLA-Cw4-SF9-restricted CTL clones were generated from HIV-infected individual and evaluated their killing activity against target cells pulsed with various concentrations of SF9 (◆–◆), SL9(■–■) or TF9 (▲–▲).

Surface plasmon resonance (SPR) analysis was used to determine equilibrium-binding affinities of HLA-Cw4 to KIR2DL1. HLA-Cw4 monomers folded with three different peptides were used. HLA-Cw4 QL9, HLA-Cw4 SF9 and HLA-Cw4 SL9 were each immobilized in one of four flow cells; the fourth flow cell contained bovine serum albumin (BSA) and served as a control. A range of concentrations from 168 down to 1 μmol/l of KIR2DL1 or KIR2DL3 were passed through all four flow cells at a rate of 10 μl/min. The K_D values were determined using equilibrium-binding curves and Scatchard analysis of equilibrium binding. No significant affinity binding of any of the HLA-Cw4 monomers to the KIR2DL3 receptor was observed. HLA-Cw4 molecules expressing the HIV gp120 peptide wild-type epitope SF9 bound to KIR2DL1 with a K_D of 23 μmol/l, which is within the range of typical cell–cell recognition events. On the other hand, the KIR2DL1 binding of HLA-Cw4 with the HIV peptide variant SL9 exhibited several times higher affinity ($K_D = 4.4$ μmol/l) than that of SF9, comparable with the Cw4 consensus peptide QL9 ($K_D = 3.5$ μmol/l) (Fig. 2a–d).

Human leukocyte antigen-Cw4-SL9 tetramers also bind to KIR2DL1 on an natural killer cell line

To confirm the binding of the HLA-Cw4 tetramer assembled with the SL9 peptide variants to KIR2DL1 naturally expressed on NK cells, an NK cell line was generated and stained with HLA-Cw4 refolded with either the SL9 or SF9 peptides. An HLA-Cw4-SF9-restricted CTL clone was also stained with the same SF9 and SL9 tetramers. As expected, the CTL clone showed better recognition of the SF9 compared with the SL9 tetramer (Fig. 2e), in keeping with the CTL lysis assays in which very low concentrations of the SF9 peptide could sensitize targets for lysis by HLA-Cw4-SF9-restricted CTL clones.

The expression of KIR2DL1 on the NK line was determined by staining with an antibody to KIR2DL1 (HP3E4), as shown in Fig. 2f. Similar to the results from the BIAcore study, the HLA-Cw4-SL9 tetramer could bind to KIR2DL1 on NK cell lines and the binding was abrogated by specific antibody. In contrast, only very weak binding was observed when the NK cell line was stained with the HLA-Cw4-SF9 index peptide tetramer (Fig. 2g).

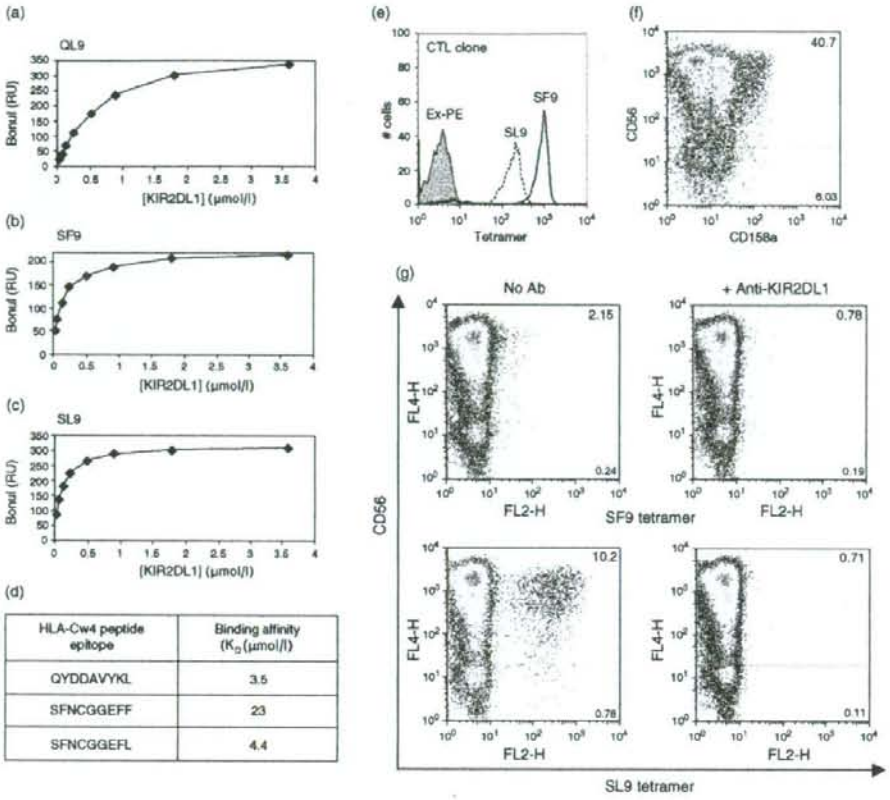

HLA-Cw4 peptide epitope	Binding affinity (K_D (μmol/l))
QYDDAVYKL	3.5
SFNCGGEFF	23
SFNCGGEFL	4.4

Fig. 2. Binding of human leukocyte antigen (HLA)-Cw4 assembled with HIV-1 gp120 peptides to KIR2DL1 was assessed by surface plasmon resonance (SPR) and tetramer staining. A range of concentrations from 168 down to 1 μmol/l of KIR2DL1 was passed through flow cells immobilized with HLA-Cw4 QL9 (a), HLA-Cw4 SF9 (b) and HLA-Cw4 SL9 (c) at a rate of 10 μl/min. The K_D values were determined using equilibrium binding curves and Scatchard analysis of equilibrium binding (d). CTL clone and natural killer (NK) cell lines were stained with HLA-Cw4 refolded with SF9 and SL9 peptides. (e) Staining of HLA-Cw4-restricted cytotoxic T lymphocyte (CTL) clone with HLA-Cw4-SF9 and HLA-Cw4-SL9 tetramer (f) Expression of KIR2DL1 on NK cell line (g) Staining of NK cell line with HLA-Cw4-SF9 (upper panel) and HLA-Cw4-SL9 tetramer (lower panel) in the absence and presence of anti-KIR2DL1.

Discussion

Our data demonstrated that while HLA-Cw4-restricted T cells respond most efficiently to the index sequence of the gp120 SF9 peptide, the T-cell escape variant forms a better ligand for KIR2DL1 when bound to HLA-Cw4.

The selective downregulation of HLA class I by HIV-1 regulatory proteins has been shown to confer some resistance to HLA-A and HLA-B-restricted CTL lysis for the infected cell [6]. A recent study by Adnan *et al.* [20] indicated that recognition of infected cells by HLA-C-restricted CTLs was unaffected by HIV-1 Nef expression, consistent with the ability of Nef to downregulate cell-surface HLA-A and HLA-B but not HLA-C molecules. As a consequence, HLA-C-restricted CTL responses may play a particularly important role in HIV-1 infection. Consistent with this hypothesis is the recent report that a single nucleotide polymorphism, which is known to lead to increased HLA-C expression on the cell surface, is associated with delayed disease progression in HIV-1 infection [14]. We have observed the HLA-Cw4-restricted response to the gp120 SF9 peptide to be immunodominant in both European and African participants and noted that this was the only CTL response that could be detected in one long-term nonprogressor (LTNP) donor (Makadzange *et al.*, in preparation). Taken together, selective downregulation of HLA class I A and B molecules provides a mechanism by which HIV-1-infected cells are able to maintain resistance to lysis by the majority of CTLs and NK cells, and hence establish a pool of long-lived infected cells in chronic HIV-1 infection.

HLA-C-restricted CTLs are, therefore, to provide strong selection pressure on the virus that would be likely to lead to the emergence of variants that escape CTL recognition. In this study, we show that the naturally occurring variant of the HLA-Cw4-restricted HIV-1 gp120 epitope SL9 represents an escape variant for wild-type SF9-specific HLA-Cw4-restricted CTL clones; this variant has been detected in patients with HLA-Cw4 (Makadzange *et al.*, in preparation). However, this variant apparently provides the virus with an additional selective advantage, through its ability to bind significantly more strongly to the NK inhibitory receptor KIR2DL1. It is plausible that this peptide variant has been selected during viral evolution because it enables infected cells to escape simultaneously from CTL and NK recognition – a phenomenon of 'double escape'.

Acknowledgement

We are very grateful to the donors who gave blood for this study. We thank Drs Peter Parham and Andrew McMichael for helpful discussion. We also thank Yuko Fukunaga for technical assistance. H.T., S.R.J. and T.D. prepared the manuscript. H.T., T.M., S.R.J. and T.D. designed the experiment. H.T., T.M., K.M., K.K. and Y.C.P. performed the experiment. C.C. provided clinical sample.

The present work was funded by the Medical Research Council, UK and the Ministry of Education, Culture, Sports, Science and Technology of Japan. H.T. was funded by the Royal Thai Government.

References

1. McMichael AJ, Rowland-Jones SL. **Cellular immune responses to HIV.** *Nature* 2001; **410**:980–987.
2. Gandhi RT, Walker BD. **Immunologic control of HIV-1.** *Annu Rev Med* 2002; **53**:149–172.
3. Lieberman J, Shankar P, Manjunath N, Andersson J. **Dressed to kill? A review of why antiviral CD8 T lymphocytes fail to prevent progressive immunodeficiency in HIV-1 infection.** *Blood* 2001; **98**:1667–1677.
4. Cohen GB, Gandhi RT, Davis DM, Mandelboim O, Chen BK, Strominger JL, Baltimore D. **The selective downregulation of class I major histocompatibility complex proteins by HIV-1 protects HIV-infected cells from NK cells.** *Immunity* 1999; **10**:661–671.
5. Williams M, Roeth JF, Kasper MR, Fleis RI, Przybycin CG, Collins KL. **Direct binding of human immunodeficiency virus type 1 Nef to the major histocompatibility complex class I (MHC-I) cytoplasmic tail disrupts MHC-I trafficking.** *J Virol* 2002; **76**:12173–12184.
6. Collins KL, Chen BK, Kalams SA, Walker BD, Baltimore D. **HIV-1 Nef protein protects infected primary cells against killing by cytotoxic T lymphocytes.** *Nature* 1998; **391**:397–401.
7. Lanier LL. **NK cell recognition.** *Annu Rev Immunol* 2005; **23**:225–274.
8. Boyington JC, Sun PD. **A structural perspective on MHC class I recognition by killer cell immunoglobulin-like receptors.** *Mol Immunol* 2002; **38**:1007–1021.
9. Valiante NM, Uhrberg M, Shilling HG, Lienert-Weidenbach K, Arnett KL, D'Andrea A, *et al.* **Functionally and structurally distinct NK cell receptor repertoires in the peripheral blood of two human donors.** *Immunity* 1997; **7**:739–751.
10. Hansasuta P, Dong T, Thananchai H, Weekes M, Willberg C, Aldemir H, *et al.* **Recognition of HLA-A3 and HLA-A11 by KIR3DL2 is peptide-specific.** *Eur J Immunol* 2004; **34**:1673–1679.
11. Thananchai H, Gillespie G, Martin MP, Bashirova A, Yawata N, Yawata M, *et al.* **Cutting edge: allele-specific and peptide-dependent interactions between KIR3DL1 and HLA-A and HLA-B.** *J Immunol* 2007; **178**:33–37.
12. Johnson RP, Trocha A, Buchanan TM, Walker BD. **Recognition of a highly conserved region of human immunodeficiency virus type 1 gp120 by an HLA-Cw4-restricted cytotoxic T-lymphocyte clone.** *J Virol* 1993; **67**:438–445.
13. Kozlowska A, Gorczyca W, Mackiewicz Z, Wojciechowska I, Kusnierczyk P. **Octapeptide but not nonapeptide from HIV-1 p24gag protein upregulates cell surface HLA-C expression.** *HIV Med* 2000; **1**:200–204.
14. Fellay J, Shianna KV, Ge D, Colombo S, Ledergerber B, Weale M, *et al.* **A whole-genome association study of major determinants for host control of HIV-1.** *Science* 2007; **317**: 944–947.
15. Fauci AS, Mavilio D, Kottilil S. **NK cells in HIV infection: paradigm for protection or targets for ambush.** *Nat Rev Immunol* 2005; **5**:835–843.
16. Alter G, Altfeld M. **NK cell function in HIV-1 infection.** *Curr Mol Med* 2006; **6**:621–629.
17. Dong T, Stewart-Jones G, Chen N, Easterbrook P, Xu X, Papagno L, *et al.* **HIV-specific cytotoxic T cells from long-term survivors select a unique T cell receptor.** *J Exp Med* 2004; **200**: 1547–1557.
18. Fan QR, Long EO, Wiley DC. **Crystal structure of the human natural killer cell inhibitory receptor KIR2DL1-HLA-Cw4 complex.** *Nat Immunol* 2001; **2**:452–460.
19. Rajagopalan S, Long EO. **The direct binding of a p58 killer cell inhibitory receptor to human histocompatibility leukocyte antigen (HLA)-Cw4 exhibits peptide selectivity.** *J Exp Med* 1997; **185**:1523–1528.
20. Adnan S, Balamurugan A, Trocha A, Bennett MS, Ng HL, Ali A, *et al.* **Nef interference with HIV-1-specific CTL antiviral activity is epitope specific.** *Blood* 2006; **108**:3414–3419.

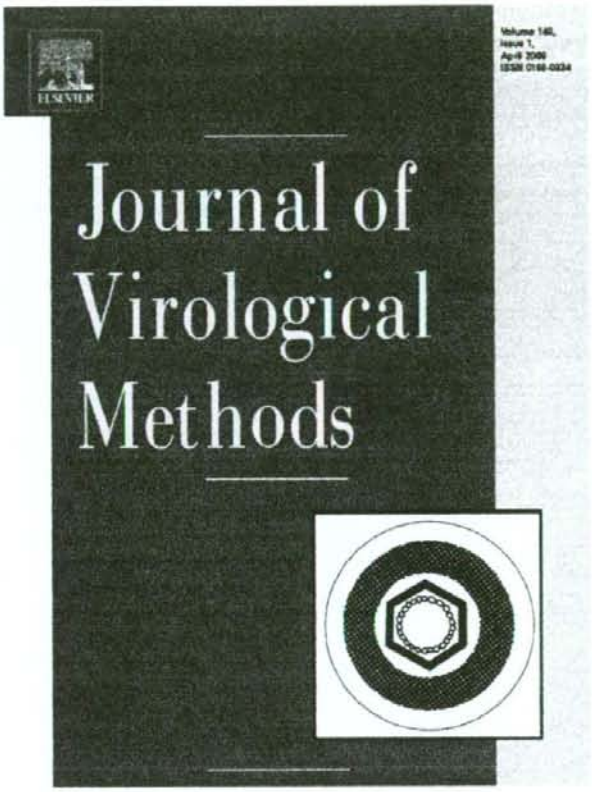

Available online at www.sciencedirect.com
ScienceDirect
Journal of Virological Methods 149 (2008) 171–174
Journal of Virological Methods
www.elsevier.com/locate/jviromet

Short communication

Homogeneous sugar modification improves crystallization of measles virus hemagglutinin

Takao Hashiguchi [a], Mizuho Kajikawa [b], Nobuo Maita [b], Makoto Takeda [a], Kimiko Kuroki [b], Kaori Sasaki [b], Daisuke Kohda [b], Yusuke Yanagi [a], Katsumi Maenaka [b,*]

[a] *Department of Virology, Faculty of Medicine, Kyushu University, 3-1-1 Maidashi, Higashi-ku, Fukuoka, Fukuoka 812-8582, Japan*
[b] *Division of Structural Biology, Medical Institute of Bioregulation, Kyushu University, 3-1-1 Maidashi, Higashi-ku, Fukuoka, Fukuoka 812-8582, Japan*

Received 15 October 2007; received in revised form 19 December 2007; accepted 10 January 2008
Available online 4 March 2008

Abstract

Measles virus (MV) enters cells by binding to the signaling lymphocyte activation molecule (also called CD150) on the cell surface, and thus shows the lymphotropism and immunosuppressive effects. The head domain (residues Asp^{149} to Arg^{617}) of the MV hemagglutinin (MV-H), the attachment protein, was produced using a transient expression system in HEK293T cells. The purified MV-H protein was heterogeneous because of a variety of complex-sugar modifications. The complex-sugar-type MV-H was crystallized successfully, and the crystals belonged to the space group P41212 with the unit cell dimension of $a = b = 134$ Å, $c = 100$ Å, but diffracted only to 3.0 Å resolution. MV-H was also expressed in HEK293SGnTI(−) cells lacking the *N*-acetylglucosaminyltransferase I activity, which render N-linked glycans of the proteins restricted and homogeneous, producing the oligomannose, $Man_5GlcNAc_2$. The native and selenomethionyl derivative proteins of the oligomannose-type MV-H were crystallized, and the native crystals well diffracted to 2.6 Å resolution. Thus, homogeneous sugar modification may be useful for improved crystallization of heavily sugar-modified viral envelope proteins.

Keywords: Measles virus; Hemagglutinin; Crystallization; Restricted *N*-glycosylation; HEK293S-GnTI(−) cells; HEK293T cells

Measles virus (MV) is an enveloped virus with a non-segmented negative-strand RNA genome and a member of the *Morbillivirus* genus in the *Paramyxoviridae* family (Lamb and Parks, 2007). MV continues to be a major killer of children, still responsible for 4% of deaths in children younger than 5 years of age worldwide (Bryce et al., 2005). MV infection causes profound immunosuppression, which makes measles patients susceptible to secondary infections accounting for high morbidity and mortality (Griffin, 2007).

MV possesses two envelope glycoproteins, the hemagglutinin (MV-H) and fusion protein, which are responsible for receptor binding and membrane fusion, respectively. Many paramyxoviruses use sialic acid as a receptor, whereas MV does not recognize sialic acid, and instead binds to the signaling lymphocyte activation molecule (SLAM, also called CD150), a membrane glycoprotein expressed on immature thymocytes, activated lymphocytes, macrophages and dendritic cells, to enter cells (Tatsuo et al., 2000; Yanagi et al., 2006). This explains both the tropism and immunosuppressive properties of MV (Yanagi et al., 2006).

The Edmonston strain of MV was isolated in 1954 from a patient with measles by using a primary culture of human kidney cells (Enders and Peebles, 1954). Currently used live attenuated MV vaccines, which are safe and very effective, were obtained by passaging this original isolate many times in a variety of cell types, including primary human kidney and amnion cells and chicken embryo fibroblasts. The Edmonston vaccine strain has acquired the ability to bind to CD46 expressed ubiquitously during the passage, although clinical isolates of MV do not usually use CD46 as a receptor (Yanagi et al., 2006).

Recently, several expression methods were developed to produce glycoproteins suitable for crystallization, which aim to achieve homogeneous sugar modification with or without the treatment with endoglycosidase H or related enzymes (Aricescu

* Corresponding author. Tel.: +81 92 642 6969; fax: +81 92 642 6764.
E-mail address: kmaenaka@bioreg.kyushu-u.ac.jp (K. Maenaka).

0166-0934/$ – see front matter © 2008 Elsevier B.V. All rights reserved.
doi:10.1016/j.jviromet.2008.01.008

et al., 2006; Chang et al., 2007). The production, crystallization and preliminary X-ray diffraction analysis of MV-H proteins produced using expression systems in two HEK293 lineage cell lines are described.

MV-H is a type II integral membrane protein that contains an N-terminal cytoplasmic tail, a single transmembrane domain, a membrane-proximal stalk domain, and a large C-terminal head domain. The head domain, which is responsible for binding to cellular receptors SLAM and CD46, comprises of Asp149 to Arg617. The gene encoding the head domain of MV-H was amplified by PCR using the p(+)MV2A (a gift from M. A. Billeter) which encodes the antigenomic full-length cDNA of the MV Edmonston strain (Radecke et al., 1995) as a template, 5′-TGG ACC GGT GAT TAT GAT CAA TAC TGT GCA-3′ as a forward primer and 5′-GTT GGT ACC TCT GCG ATT GGT TCC ATC TTC-3′ as a reverse primer. The amplified fragment was digested with restriction enzymes, AgeI and KpnI, and cloned into the pHLsec vector (Aricescu et al., 2006) to add the N-terminal signal sequence and C-terminal His^6 tag to the protein-coding sequence. Then, the plasmid was digested with EcoRI and XhoI, and the fragment was cloned into the pCA7 vector (Takeda et al., 2005). The resultant plasmid (designated as pCA7sec-MV-H) contains the SV40 replication origin and the protein expression level can be increased by co-transfection with the expression plasmid encoding the SV40 large T antigen (pCA7-SV40).

To produce the complex-sugar-type MV-H, HEK293T cells were transiently transfected with pCA7sec-MV-H and pCA7-SV40 using polyethyleneimine. To express the oligomannose-type MV-H, the same transient transfection was performed using HEK293SGnTI(−) cells (Reeves et al., 2002), which are devoid of the N-acetylglucosaminyltransferase I (GnTI) activity and render N-linked glycans restricted and homogeneous, producing the oligomannose. $Man_5GlcNAc_2$. This cell line was employed to increase a chance of successful crystallization of sugar-modified proteins, whose heterogeneous sugars usually inhibit crystallization (Aricescu et al., 2006; Chang et al., 2007). Plasmid vectors were transfected into 90% confluent HEK293T or HEK293SGnTI(−) cells with the ratio of 1.0:1.5 (DNA:polyethyleneimine) in Dulbecco's modified Eagle's medium (DMEM) (MP Biomedicals Inc.) containing 2% fetal calf serum (FCS) (Invitrogen). The concentration of FCS was increased to 2% immediately after mixing the plasmid and polyethyleneimine in DMEM without FCS. The cells were cultured in roller bottles (total surface area, 850 cm^2). About 2 mg of the oligomannose-type protein and 1.2 mg of the complex-sugar-type one were obtained from 15 roller bottles of HEK293SGnTI(−) and HEK293T cells, respectively. The selenomethionyl (SeMet) derivative of the oligomannose-type MV-H was

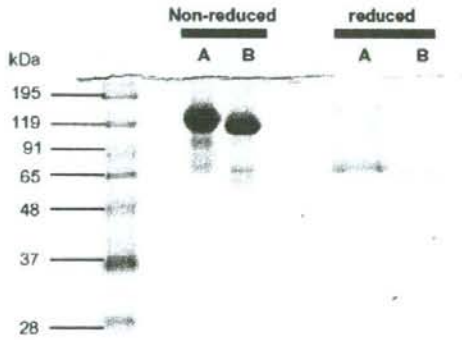

Fig. 1. SDS-PAGE and Western blot of MV-H proteins. (A) Complex-sugar-type MV-H expressed in HEK293T cells. (B) Oligomannose-type MV-H expressed in HEK293SGnTI(−) cells. Under non-reducing condition, MV-H proteins exhibited 140 kDa and 120 kDa in molecular weights (MWs), respectively. The difference in MWs was due to the difference in N-linked sugar modification between HEK293T (complex-sugar) and HEK293SGnTI(−) (oligomannose) cells. Under reducing condition, MV-H proteins exhibited 70 kDa and 60 kDa, respectively.

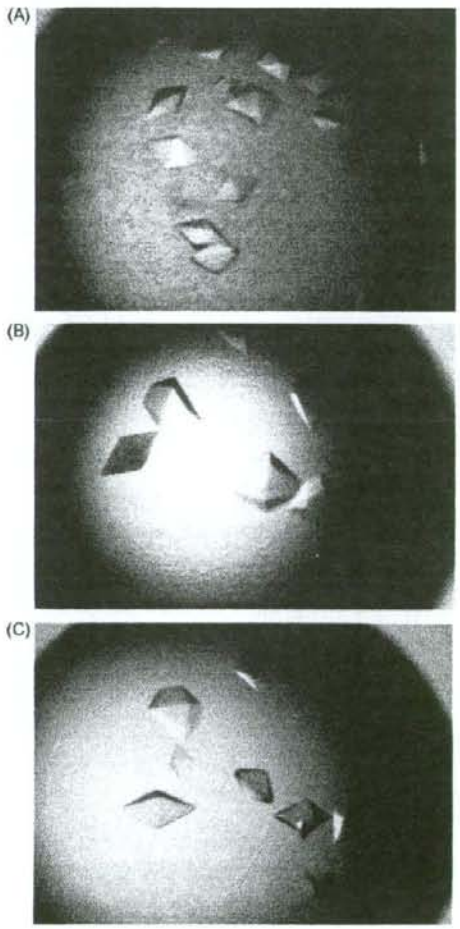

Fig. 2. MV-H protein crystals by the hanging drop vapor diffusion. (A) Complex-sugar-type MV-H crystals expressed in HEK293T cells at 293 K. (B) Oligomannose-type MV-H crystals expressed in HEK293SGnTI(−) cells at 293 K. (C) Ser-Met oligomannose-type MV-H crystals expressed in HEK293SGnTI(−) cells at 303 K with constant shaking.

expressed in the similar way to the native oligomannose-type MV-H in DMEM supplemented with L-selenomethionine (30 mg/l in culture) in place of L-methionine.

The supernatant containing the soluble MV-H protein was collected at 4 days post-transfection. It was mixed with the one-tenth amount of the 10× Ni-NTA column binding buffer (500 mM NaH_2PO_4 pH8.0, 1.5 M NaCl, 100 mM imidazole) and incubated at 277 K overnight. The mixture was centrifuged at 5500 × *g* at 277 K for 10 min and the supernatant was filtrated through 0.22 μm filter. Subsequently, the solution containing the His^6-tagged MV-H protein was loaded onto the Ni-NTA column. It was washed with 20 column volumes of the wash buffer (50 mM NaH_2PO_4 pH 8.0, 150 mM NaCl, 10 mM imidazole) and then eluted by the elution buffer (50 mM NaH_2PO_4 pH 8.0, 150 mM NaCl, 500 mM imidazole). The eluted sample was purified further by size-exclusion chromatography (superdex 200GL 10/300 (Amersham Biosciences)) equilibrated with the running buffer (20 mM Tris–HCl pH 8.0 and 100 mM NaCl). The purified MV-H protein was analyzed by SDS-PAGE with Coomassie brilliant blue. The complex-sugar-type MV-H was more heterogeneous than the oligomannose-type (Fig. 1).

Initial crystallization screenings for the complex-sugar- and the oligomannose-type MV-H were performed by the sitting drop vapor diffusion techniques with the Intelli-Plate 96 well crystallization plate (Hampton Research) and the Hydra Plus One crystallization robot (Matrix Technologies Corporation). Several commercially available screen kits were used; Crystal Screen and Crystal Screen II (Hampton Research), Wizard 1 and Wizard 2 (Emerald Biostructures), and the Nextal series (The Classics Suite, The Classic Lite Suite, The $AmSO_4$, The Sparse Matrix 1 and The Sparse Matrix 2) (Nextal Biotechnologies). The drop was a mixture of 0.2 μl of protein solution and 0.2 μl of reservoir solution, and the crystallization plates were incubated at 293 K.

Crystals of the native complex-sugar-type MV-H protein were obtained with Crystal Screen I solution No. 34 (100 mM sodium acetate trihydrate, pH 4.6, 2.0 M sodium formate), The Sparse Matrix 1 solution No. 53 (200 mM magnesium chloride, 100 mM sodium cacodyrate, pH 6.5, 10% PEG3000) or No. 70 (200 mM sodium chloride, 100 mM Na/K phosphate, pH 6.2, 10% PEG8000). After optimization, the crystals were grown by the hanging drop vapor diffusion at 293 K from the mixture containing 1 μl of protein (8.4 mg/ml, in 20 mM Tris–HCl, pH 8.0, 100 mM NaCl) and 1 μl of mother liquor (200 mM NaCl, 100 mM sodium cacodylate, pH 6.5, 10% polyethylene glycol 8000) (Fig. 2A). The crystals diffracted only to 3.0 Å resolution at beamline BL41XU of Spring8 (Harima, Japan). The diffraction data were autoindexed, integrated and scaled with HKL2000 program package (Otwinowski and Minor, 1997) and indicated the space group $P4_12_12$, with unit cell dimensions of $a = 134$ Å, $b = 134$ Å, $c = 100$ Å ($R_{merge} = 9.4\%$ on data to 3.0 Å resolution, data completeness = 99.6%) and contained one MV-H protein per asymmetric unit (Table 1).

On the other hand, crystals of the native oligomannose-type MV-H protein were obtained with Crystal Screen I solution No. 34, The Sparse Matrix 1 solution No. 14 (100 mM sodium cacodyrate, pH 6.5, 1.26 M ammonium sulfate), No. 53, No. 70 or No. 87 (200 mM zinc acetate, 100 mM imidazole, pH 8.0, 2.5 M sodium chloride). Further refinement of crystallization conditions was performed. Finally, the crystals were grown by the hanging drop vapor diffusion at 293 K from the drops containing 1 μl each of protein (9.7 mg/ml, in 20 mM Tris–HCl, pH 8.0, 100 mM NaCl) and mother liquor (100 mM sodium acetate trihydrate, pH 4.6, 2.0 M sodium formate, 10% ethylene glycol) (Fig. 2B). Crystals of the native oligomannose-type MV-H became suitable for cryo-experiment by increasing the concentration of ethylene glycol to 30%. A diffraction data set was collected to 2.6 Å resolution at 100 K, from the single largest

Table 1
Crystallographic data statistics[a]

	SeMet (oligomannose)	Native (oligomannose)	Native (complex-sugar)
Data collection			
Space group	$P4_12_12$	$P4_12_12$	$P4_12_12$
Unit cell parameters (Å)			
$a = b$	134.59	134.09	134.55
c	100.26	100.75	99.24
Wavelength (Å)	0.9790 (peak)	0.9780	1.0000
Resolution range (Å)	30–2.85 (2.99–2.85)	30–2.6 (2.69–2.6)	30–3.0 (3.11–3.0)
No. of measured reflections	1,018,485	346,891	131,668
No. of unique reflections	22,022	28,691	18,727
Completeness (%)	99.9 (99.9)	99.2 (99.9)	99.6 (98.1)
Multiplicity	46.2 (45.9)	12.1 (12.2)	7.0 (6.4)
R_{sym}[b]	0.096 (0.459)	0.080 (0.644)	0.094 (0.388)
$I/\sigma I$	7.2 (1.7)	11.6 (4.3)	9.4 (5.11)
Mosaicity (°)	0.49	0.23	0.73
Molecules per AU	1	1	1
Phasing statistics			
Se sites (found/all)	9/13		
Figure of merit (after SOLVE/after RESOLVE)	0.401/0.711		

[a] Highest resolution shell is shown in parenthesis.
[b] $R_{sym} = \Sigma|I_i - \langle I_i \rangle|/\Sigma I_i$, where I_i is the observed intensity and $\langle I_i \rangle$ is the average intensity obtained from multiple observations of symmetry-related reflections.

crystal, at beamline BL41XU or BL38B2 of Spring8 (Harima, Japan). Thus, homogeneous sugar modification seems to assist the production of well-diffracted protein crystals.

Although the SeMet derivative MV-H was crystallized under the same condition as the native MV-H, the diffraction was not sufficient for structure determination. The extensive crystallization screening was thus done using the screen kits. Crystals of the SeMet derivative were obtained successfully in the condition of 200 mM NaCl, 100 mM Na/K phosphate, pH 6.2, 7% polyethylene glycol 8000 by the hanging drop vapor diffusion at 303 K with constant shaking (Fig. 2C). Crystals of the SeMet oligomannose-type MV-H became suitable for cryo-experiment by increasing the concentration of glycerol to 30%. A diffraction data set was collected to 2.85 Å resolution at 100 K, from the single largest crystal, at beamline BL6A at Photon Factory (Tsukuba, Japan). Crystals of the native and SeMet forms of the oligomannose-type MV-H belonged to the same space group and similar unit cell dimension as the native complex-sugar-type MV-H.

A search for Se-atom sites was carried out with SOLVE (Terwilliger and Berendzen, 1999), resulting in 9 out of 13 Se sites. Phases were further improved by density-modification methods using RESOLVE (Terwilliger, 2000), with a mean figure-of-merit of 0.711. The statistics of data collection and phasing are summarized in Table 1. The resulting electron-density map allowed tracing of the main chains of the polypeptides. Model building and structure refinement were successful (Hashiguchi et al., 2007).

In conclusion, the complex-sugar-type MV-H was crystallized successfully, but the regulated sugar modification without the Endo-H treatment produced homogeneous oligomannose-modified MV-H proteins, which provided better-diffracted crystals. Thus, homogeneous sugar modification may be useful for improved crystallization of heavily sugar-modified viral envelope proteins.

Acknowledgements

We thank S. Wakatsuki, N. Igarashi, N. Matsugaki, M. Kawamoto, H. Sakai, N. Shimizu, and K. Hasegawa for assistance in data collection at the Photon Factory and SPring-8. We also thank A. Aricescu and E.Y. Jones for helping the expression using HEK293 cells. This work was supported in part by the Ministry of Education, Culture, Sports, Science and Technology and the Ministry of Health, Labor and Welfare of Japan, and the Japan Bio-oriented Technology Research Advancement Institute (BRAIN).

References

Aricescu, A.R., Assenberg, R., Bill, R.M., Busso, D., Chang, V.T., Davis, S.J., Dubrovsky, A., Gustafsson, L., Hedfalk, K., Heinemann, U., Jones, I.M., Ksiazek, D., Lang, C., Maskos, K., Messerschmidt, A., Macieira, S., Peleg, Y., Perrakis, A., Poterszman, A., Schneider, G., Sixma, T.K., Sussman, J.L., Sutton, G., Tarboureich, N., Zeev-Ben-Mordehai, T., Jones, E.Y., 2006. Eukaryotic expression: developments for structural proteomics. Acta Crystallogr. D: Biol. Crystallogr. 62, 1114–1124.

Bryce, J., Boschi-Pinto, C., Shibuya, K., Black, R.E., 2005. WHO estimates of the causes of death in children. Lancet 365, 1147–1152.

Chang, V.T., Crispin, M., Aricescu, A.R., Harvey, D.J., Nettleship, J.E., Fennelly, J.A., Yu, C., Boles, K.S., Evans, E.J., Stuart, D.I., Dwek, R.A., Jones, E.Y., Owens, R.J., Davis, S.J., 2007. Glycoprotein structural genomics: solving the glycosylation problem. Structure 15, 267–273.

Enders, J.F., Peebles, T.C., 1954. Propagation in tissue cultures of cytopathogenic agents from patients with measles. Proc. Soc. Exp. Biol. Med. 86, 277–286.

Griffin, D.E., 2007. Measles virus. In: Knipe, P.M.H.D.M., Griffin, D.E., Lamb, R.A., Martin, M.A., Roizman, B., Straus, S.E. (Eds.), Fields Virology, 5th ed. Lippincott Williams & Wilkins, Philadelphia, pp. 1551–1585.

Hashiguchi, T., Kajikawa, M., Maita, N., Takeda, M., Kuroki, K., Sasaki, K., Kohda, D., Yanagi, Y., Maenaka, K., 2007. Crystal structure of measles virus hemagglutinin provides insight into effective vaccines. Proc. Natl. Acad. Sci. U.S.A. 104, 19535–19540.

Lamb, R.A., Parks, G.D., 2007. Paramyxoviridae: the viruses and their replication. In: Knipe, P.M.H.D.M., Griffin, D.E., Lamb, R.A., Martin, M.A., Roizman, B., Straus, S.E. (Eds.), Fields Virology, 5th ed. Lippincott Williams & Wilkins, Philadelphia, pp. 1449–1496.

Otwinowski, Z., Minor, W., 1997. Processing of X-ray diffraction data collected in oscillation mode. Methods Enzymol. 276, 307–326.

Radecke, F., Spielhofer, P., Schneider, H., Kaelin, K., Huber, M., Dotsch, C., Christiansen, G., Billeter, M.A., 1995. Rescue of measles viruses from cloned DNA. EMBO J. 14, 5773–5784.

Reeves, P.J., Callewaert, N., Contreras, R., Khorana, H.G., 2002. Structure and function in rhodopsin: high-level expression of rhodopsin with restricted and homogeneous *N*-glycosylation by a tetracycline-inducible *N*-acetylglucosaminyltransferase I-negative HEK293S stable mammalian cell line. Proc. Natl. Acad. Sci. U.S.A. 99, 13419–13424.

Takeda, M., Ohno, S., Seki, F., Nakatsu, Y., Tahara, M., Yanagi, Y., 2005. Long untranslated regions of the measles virus M and F genes control virus replication and cytopathogenicity. J. Virol. 79, 14346–14354.

Tatsuo, H., Ono, N., Tanaka, K., Yanagi, Y., 2000. SLAM (CDw150) is a cellular receptor for measles virus. Nature 406, 893–897.

Terwilliger, T.C., 2000. Maximum-likelihood density modification. Acta Crystallogr. D: Biol. Crystallogr. 56 (Pt 8), 965–972.

Terwilliger, T.C., Berendzen, J., 1999. Automated MAD and MIR structure solution. Acta Crystallogr. D: Biol. Crystallogr. 55 (Pt 4), 849–861.

Yanagi, Y., Takeda, M., Ohno, S., 2006. Measles virus: cellular receptors, tropism and pathogenesis. J. Gen. Virol. 87, 2767–2779.

Available online at www.sciencedirect.com
ScienceDirect
Biochimica et Biophysica Acta 1784 (2008) 621–628
www.elsevier.com/locate/bbapap

Serotriflin, a CRISP family protein with binding affinity for small serum protein-2 in snake serum

Narumi Aoki [a], Akie Sakiyama [a], Kimiko Kuroki [b], Katsumi Maenaka [b], Daisuke Kohda [b], Masanobu Deshimaru [a,*], Shigeyuki Terada [a]

[a] *Department of Chemistry, Faculty of Science, Fukuoka University, 8-19-1 Nanakuma, Jonan-ku, Fukuoka 814-0180, Japan*
[b] *Division of Structural Biology, Medical Institute of Bioregulation, Kyushu University, 3-1-1 Maidashi, Higashi-ku, Fukuoka 812-8582, Japan*

Received 5 September 2007; received in revised form 18 December 2007; accepted 24 December 2007
Available online 5 January 2008

Abstract

Habu (*Trimeresurus flavoviridis*) serum contains 3 small serum proteins (SSP-1, SSP-2, and SSP-3) with molecular masses of 6.5 to 10 kDa. Gel filtration analysis showed that all the SSPs exist in high molecular mass forms of approximately 60 kDa in the serum. Ultrafiltration of Habu serum showed that SSPs dissociated from the complex below a pH of 4. An SSP-binding protein was purified from Habu serum by gel filtration, ion exchange, and reverse-phase HPLC. N-terminal sequencing yielded a 39-amino acid sequence, similar to the N-terminal region of triflin, which is a snake venom-derived Ca^{2+} channel blocker that suppresses smooth muscle contraction. The amino acid sequence of this protein, termed serotriflin, was established by peptide analysis and cDNA cloning. Serotriflin is a glycosylated protein and consists of 221 amino acids. Among the 3 SSPs, only SSP-2 formed a noncovalent complex with serotriflin. It was bound to triflin and serotriflin with high affinity, as evidenced by surface plasmon resonance. SSP-2 is considered to be a protein that prevents self injury by accidental leaking of venom into the blood.

Keywords: CRISP; PSP94; SSP; Snake serum; Triflin; *Trimeresurus flavoviridis*

1. Introduction

The human prostatic secretory protein of 94 amino acids (PSP94) is a 10.7-kDa, nonglycosylated, cysteine-rich protein [1], and the homologous proteins have also been identified in several mammals [2–4] and ostrich [5]. In addition to the 10 conserved cysteine residues that form 5 disulfide bonds, there are only 16 amino acids conserved across all the mammalian proteins, suggesting that they evolved at a relatively rapid rate with few constraints of the selection pressure [6].

Recently, we isolated a novel low molecular mass protein from the serum of Habu (*Trimeresurus flavoviridis*) and termed this protein small serum protein (SSP) [7]. Analysis of the N-terminal residues indicated that SSP belongs to the PSP94 protein family, despite the low sequence homology, since the cysteine residues of these proteins were topologically similar. We also found 2 similar proteins (SSP-2 and SSP-3) in the same serum, and the first SSP was then renamed SSP-1. SSPs are the first PSP94 family proteins to be found in reptiles.

SSP-1 showed an inhibitory effect against brevilysin H6 [8], a snake venom metalloproteinase with weak hemorrhagic activity. SSP-3 also exhibited a slight inhibition of brevilysin H6. On the other hand, SSP-2 demonstrated a strong binding affinity for triflin, which was isolated from *T. flavoviridis* venom as the protein responsible for blocking smooth muscle contraction and belongs to the cysteine-rich secretory protein (CRISP) family [9]. This suggests that SSP-2 exists in snake blood for defense against the toxic effects of venom in case of accidental self-envenomation. To our knowledge, SSP-2 is the

Abbreviations: CRISP, cysteine-rich secretory protein; MALDI-TOF-MS, matrix-assisted laser desorption ionization time-of-flight mass spectrometry; P_{40}, 60%; ammonium sulfate fraction; PSP94, prostatic secretory protein of 94 amino acids; PSPBP, PSP94-binding protein; SCP, sperm coating glycoprotein; SSP, small serum protein

* Corresponding author. Tel.: +81 92 871 6631; fax: +81 92 865 6030.
E-mail address: deshi@fukuoka-u.ac.jp (M. Deshimaru).

1570-9639/$ - see front matter © 2007 Elsevier B.V. All rights reserved.
doi:10.1016/j.bbapap.2007.12.010